AppliedMath

MDPI

Article

Mathematical Model Analysis for the Dynamics and Control of Malaria and Typhoid Fever Co-Infection

Obiora Cornelius Collins * and Oludolapo Akanni Olanrewaju

Institute of Systems Science, Durban University of Technology, Durban 4000, South Africa; oludolapoo@dut.ac.za
* Correspondence: obiorac@dut.ac.za

Abstract

Malaria and typhoid fever co-infection produces severe illness affecting public health, especially in countries where both diseases coexist. A mathematical model that considers the critical factors influencing the transmission dynamics and control interventions of malaria and typhoid fever co-infection is developed. The essential epidemiological features of the model, such as the basic reproduction number and disease-free equilibrium, are determined and analysed. A dynamical systems analysis of the model reveals the conditions under which the disease can be eradicated or persists. Numerical simulations are conducted using real data from Nigeria as a case study. By fitting the model to the real data, essential parameter values are estimated and model prediction that reveals the possible long-term dynamics of the model is determined. The impact of the various control interventions are investigated. These findings are anticipated to aid in improving the management of malaria–typhoid co-infection in endemic regions for expeditious disease eradication.

Keywords: disease dynamics; co-infection; malaria; typhoid fever; stability analyses; model fitting; parameter estimation; model prediction

1. Introduction

Malaria is a life-threatening, mosquito-borne disease caused by Plasmodium parasites transmitted through the bite of infected female Anopheles mosquitoes. Common early symptoms of malaria are fever, headache, and chills and typically start a few weeks after an infected mosquito bite. The incubation period of malaria usually ranges from 7 to 30 days [1]. Globally in 2024, there were an estimated 282 million cases of malaria, an increase of about 9 million cases (3%) compared with 2023. The estimated number of malaria deaths stood at 610,000 in 2024 compared to 598,000 in 2023 [2]. The African region continues to carry a high share of the global malaria burden with about 95% of all malaria cases and deaths in 2024 [2]. Malaria is preventable by avoiding mosquito bites and curable using appropriate medical treatment such as Artemisinin-based Combination Therapies (ACTs) [2].

Typhoid fever is a life-threatening infection caused by the bacterium *Salmonella* Typhi [3]. Its transmission is usually through contaminated food or water [3]. Symptoms include prolonged high fever, fatigue, headache, nausea, abdominal pain, and constipation or diarrhoea [3]. Typhoid is preventable through access to safe water and adequate sanitation, hygiene among food handlers, and typhoid vaccination. Typhoid fever can be treated with antibiotics. Increasing resistance to antibiotic treatment is making it easier for typhoid to spread in communities that lack access to safe drinking water or adequate sanitation. Based on 2019 estimates, there are 9 million cases of typhoid fever annually, resulting in

Check for updates

Received: 24 July 2026
Revised: 6 September 2026
Accepted: 8 September 2026
Published: 11 September 2026

Copyright: © 2026 by the authors. Licensee MDPI, Basel, Switzerland. This article is an open access article distributed under the terms and conditions of the Creative Commons Attribution (CC BY) license.

about 110,000 deaths per year [3]. Typhoid risk is higher in populations that lack access to safe water and adequate sanitation, and children are at the highest risk [3].

Malaria and typhoid fever co-infection occurs when a person is simultaneously infected with the Plasmodium parasite (which causes malaria) and the *Salmonella* Typhi bacteria (which causes typhoid fever). Both diseases are endemic in tropical regions and can severely exacerbate each other if not treated concurrently. Co-infection is a serious public health concern due to the increased severity of symptoms and diagnosis challenges involved [3]. This study is an attempt to use a mathematical model to investigate the transmission dynamics and control interventions of malaria and typhoid fever co-infection.

Mathematical models have been successfully used to study real-life problems, such as the spread of infectious diseases [4–13]. Some of the important research findings in the literature that considered mathematical models to study malaria infections are reviewed and presented here. Kim et al. [14] used a malaria epidemiological model that incorporates climate-dependent parameters to analyze the impact of climate change on malaria transmission. Collins & Duffy [8] used a mathematical epidemiological model incorporating drug resistance, treatment, and the use of mosquito nets to analyse the transmission dynamics of malaria in Nigeria. Agusto et al. [9] used a mathematical model for malaria to investigate the impact of bed-nets. Herdicho et al. [15] used a mathematical model that incorporates seasonal factors, insecticide, and treatment to analyse the impact of variability in temperature and rainfall on malaria transmission dynamics. Other important research findings that use mathematical models to study the transmission dynamics and control measures for malaria can be found in [16–20].

Some significant research findings that considered mathematical epidemiological models to study typhoid fever infections are reviewed and presented here. For instance, ref. [21] used a deterministic mathematical model to investigate the transmission dynamics of typhoid fever with treatment and booster vaccination. A paper by [22] proposed a novel mathematical model for typhoid fever disease that incorporates the use of modern and traditional medicines as modes of treatment. Another important research finding by [23] considered numerical methods to examine the dynamical behaviour of a typhoid fever non-linear mathematical model. Research undertaken by [24] investigated a robust numerical analytic strategy for typhoid fever that takes infection protection into consideration and incorporates fuzzy parameters. Research by [25] involved the formulation of an optimal control model for the transmission dynamics of typhoid fever that included a medically hygienic compartment in the model. Their findings revealed that a combination of environmental sanitation with personal hygiene and treatment was the most efficient in controlling the spread of typhoid fever. Other important research findings that use mathematical models to study the transmission dynamics and control interventions of typhoid fever can be found in [21,25–32].

Research findings on malaria and typhoid fever co-infection are reviewed and presented here. For instance, a study by [33] on malaria–typhoid fever co-infection among febrile patients in Ngaoundéré (Adamawa, Cameroon) revealed that the two infections are more prevalent in Ngaoundéré City, particularly amongst children and women. Another study by [34] on malaria–typhoid fever co-infection using a retrospective analysis of University Hospital records in Nigeria also revealed that the prevalence of co-infection peaked in May (9.7%), followed by June (8.9%) and April (5.7%), with children aged 6–12 years exhibiting the highest co-infection rate (18.5%), while those under five had the lowest (6.3%). A study by [35] on the incidence of malaria–typhoid co-infection among the adult population in the Unwana community, Afikpo north local government area, Ebonyi state, southeastern Nigeria revealed that out of the 350 blood samples analysed, 190 (54.2%) were positive for malaria, 173 (49.4%) were positive for *Salmonella enterica* serovar Typhi, while

127 (36.2%) were positive for both typhoid and malaria. A study by [36] used a mathematical model to investigate the dynamics of malaria–typhoid co-infection, incorporating both vector and non-vector malaria transmission routes and environmental transmission for typhoid. A further study by [37] used a mathematical model describing the co-infection dynamics of malaria and typhoid to identify the distinct features of typhoid and malaria infection dynamics as well as relationships associated with their co-infection.

There is no doubt that these research findings have made significant contributions to understanding the transmission dynamics and control interventions for malaria and typhoid fever as well as their co-infection. However, none of these studies used real data to fit the mathematical models considered nor did they conduct parameter estimation from the data or conduct model prediction, which are crucial to achieve more accurate results that can improve disease management and control interventions for malaria and typhoid fever co-infection. The aim of this study is to fill this gap in the literature by formulating a mathematical model for the co-infection of malaria and typhoid fever, to use the model to conduct parameter estimation and prediction of the future dynamics of the disease, and to investigate the impact of control interventions. The results of this study are anticipated to aid in improving the management of malaria–typhoid fever co-infection in endemic regions. The remainder of this paper is organised as follows: Model development is presented in Section 2, with analyses and results presented in Section 3, Numerical simulations, including model fitting, parameter estimation, model prediction, and investigation of the impact of control measures, are described in Section 4. Finally, a discussion of the findings is presented in Section 5.

2. Model Development

Malaria is a parasitic infection transmitted through the bite of an infected female Anopheles mosquito. Malaria is treatable using Artemisinin-based combination therapy and preventable by avoiding mosquito bites. Typhoid fever is a life-threatening bacterial infection caused by *Salmonella* Typhi. It spreads primarily through contaminated food and water. Typhoid fever is treatable with antibiotics and preventable through proper hygiene, safe water access, and adequate sanitation infrastructure. Co-infection by these two diseases is possible, especially in areas where the two diseases are endemic.

A mathematical model for malaria–typhoid fever co-infection is formulated based on the following assumptions. The model comprises the human population, the female Anopheles mosquito population, and the concentration of Salmonella bacteria in food or water. The total human population $N_h(t)$ at time (t) is partitioned into eight sub-populations, namely, susceptible human population $(S(t))$, human population infected with malaria $(I_a(t))$, human population infected with typhoid fever $(I_b(t))$, human population co-infected with malaria and typhoid fever $(I_{ab}(t))$, human population on malaria treatment $(P_a(t))$, human population on typhoid fever treatment $(P_b(t))$, human population on treatment for malaria and typhoid fever co-infection $(P_{ab}(t))$, and human population that is temporally immune from malaria, typhoid fever, or both $(R(t))$. The female Anopheles mosquito population $(N_v(t))$ that hosts/transmits the malaria parasite is partitioned into two: susceptible mosquitoes $(X(t))$ and infected mosquitoes $(Y(t))$. The concentration of Salmonella bacteria in food or water is denoted by $(B(t))$.

The natures of the interactions among these variables (humans, female Anopheles mosquitoes, Salmonella bacteria in food or water) that give rise to malaria and typhoid fever co-infection dynamics are described as follows. Humans are recruited into the $S(t)$ through birth at a rate Λ_h^* and leave the class as they get infected with malaria or typhoid fever at a rate β_a^*, β_b^*, respectively. Those already infected with malaria can in addition get infected with typhoid fever, leading to co-infection at a rate β_{ab}^* and vice versa. Those infected with

malaria or typhoid fever or co-infected get treated at a rate $\sigma_a^*, \sigma_b^*, \sigma_{ab}^*$, respectively. Treated individuals for these various classes (P_a, P_b, P_{ab}) recover at a rate $\gamma_a^*, \gamma_b^*, \gamma_{ab}^*$, respectively, or are returned back to the various infected classes (I_a, I_b, I_{ab}) due to treatment failures at rate $\theta_a^*, \theta_b^*, \theta_{ab}^*$, respectively. We assume that individuals in the treatment classes P_a and P_b cannot acquire other infection. This is because treatment for individuals experiencin infection is often carried out in health facilities where patients are properly taken care of and the chances of contacting other infections are minimised. Disease-induced deaths for the infected classes (I_a, I_b, I_{ab}) occur at rates $\delta_a^*, \delta_b^*, \delta_{ab}^*$, respectively. Natural deaths occur in all human compartments at a rate μ. Humans infected (I_b) or co-infected (I_{ab}) with typhoid fever shed the pathogen into the environment at rates ν_b or ν_{ab}, respectively. The pathogens decay/die naturally or by using appropriate control measures at rates ρ or ψ, respectively.

The female Anopheles mosquito population X increases through recruitment at a rate Λ_v^* and decreases as they get infected with $I_a(t)$ or $I_{ab}(t)$ at a rate α^*. Both $X(t)$ and $Y(t)$ die naturally at a rate ξ^*. Applying insecticides or fumigation (control interventions) kill $X(t)$ and $Y(t)$ at a rate ϕ^*. One of the methods of preventing mosquito bites is by using an insecticide-treated mosquito net. This is considered by assuming that the use of insecticide-treated net reduces malaria transmission by a factor c_1. Prevention of typhoid fever is achieved through sanitation. Thus, typhoid fever transmission can be reduced by a factor c_2 due to sanitation. Based on these formulations, the following malaria and typhoid fever co-infection model with control interventions is obtained

$$\begin{aligned}
\frac{dS(t)}{dt} &= \Lambda_h^* - (1-c_1)\beta_a^* S(t)Y(t) - (1-c_2)\beta_b^* S(t)B(t) + \omega^* R(t) - \mu S(t),\\
\frac{dI_a(t)}{dt} &= (1-c_1)\beta_a^* S(t)Y(t) + \theta_a^* P_a(t) - (1-c_2)\beta_{ab}^* I_a(t)B(t) - (\mu + \sigma_a^* + \delta_a^*)I_a(t),\\
\frac{dI_b(t)}{dt} &= (1-c_2)\beta_b^* S(t)B(t) + \theta_b^* P_b(t) - (1-c_1)\beta_{ba}^* I_b(t)Y(t) - (\mu + \sigma_b^* + \delta_b^*)I_b(t),\\
\frac{dI_{ab}(t)}{dt} &= (1-c_2)\beta_{ab}^* I_a(t)B(t) + (1-c_1)\beta_{ba}^* I_b(t)Y(t) + \theta_{ab}^* P_{ab}(t) - (\mu + \sigma_{ab}^* + \delta_{ab}^*)I_{ab}(t),\\
\frac{dP_a(t)}{dt} &= \sigma_a^* I_a(t) - (\mu + \gamma_a^* + \theta_a^*)P_a(t),\\
\frac{dP_b(t)}{dt} &= \sigma_b^* I_b(t) - (\mu + \gamma_b^* + \theta_b^*)P_b(t),\\
\frac{dP_{ab}(t)}{dt} &= \sigma_{ab}^* I_{ab}(t) - (\mu + \gamma_{ab}^* + \theta_{ab}^*)P_{ab}(t),\\
\frac{dR(t)}{dt} &= \gamma_a^* P_a(t) + \gamma_b^* P_b(t) + \gamma_{ab}^* P_{ab}(t) - (\mu + \omega^*)R(t),\\
\frac{dX(t)}{dt} &= \Lambda_v^* - (1-c_1)\alpha^* X(t)(I_a(t) + I_{ab}(t)) - (\xi^* + \phi^*)X(t),\\
\frac{dY(t)}{dt} &= (1-c_1)\alpha^* X(t)(I_a(t) + I_{ab}(t)) - (\xi^* + \phi^*)Y(t),\\
\frac{dB(t)}{dt} &= \nu_b^* I_b(t) + \nu_{ab}^* I_{ab}(t) - (\rho^* + \psi^*)B(t),
\end{aligned} \tag{1}$$

with initial conditions, $S(0) \geq 0$, $I_a(0) \geq 0$, $I_b(0) \geq 0$, $I_{ab}(0) \geq 0$, $P_a(0) \geq 0$, $P_b(0) \geq 0$, $P_{ab}(0) \geq 0$, $R(0) \geq 0$, $X(0) \geq 0$, $Y(0) \geq 0$, and $B(0) \geq 0$. Descriptions of the variables and parameters for model (1) are presented in Tables 1 and 2, respectively.

Table 1. Description for variables for model (1).

Variables	Description	Unit
$N_h(t)$	Total population of humans	Humans Km^{-2}
$S(t)$	Susceptible population of humans	Humans Km^{-2}
$I_a(t)$	Humans infected with malaria	Humans Km^{-2}

Table 1. *Cont.*

Variables	Description	Unit
$I_b(t)$	Humans infected with typhoid fever	Humans Km^{-2}
$I_{ab}(t)$	Humans co-infected with malaria and typhoid fever	Humans Km^{-2}
$P_a(t)$	Humans on malaria treatment	Humans Km^{-2}
$P_b(t)$	Humans on typhoid fever treatment	Humans Km^{-2}
$P_{ab}(t)$	Humans on co-infection treatment	Humans Km^{-2}
$R(t)$	Temporal immune against malaria, typhoid fever, or both	Humans Km^{-2}
$N_v(t)$	Total population of female Anopheles mosquitoes	Vectors Km^{-2}
$X(t)$	Susceptible mosquitoes that host malaria parasite	Vectors Km^{-2}
$Y(t)$	Infected mosquitoes that transmit malaria parasite	Vectors Km^{-2}
$B(t)$	Concentration of Salmonella bacteria in food or water	Cells mL^{-1}

Table 2. Description of parameters for model (1).

Parameters	Description	Unit
Λ_h^*	Recruitment rate of humans into $S(t)$	Humans Km^{-2} $Year^{-1}$
β_a^*	Transmission rate from $S(t)$ to $I_a(t)$	Km^2 $Vector^{-1}$ $Year^{-1}$
β_b^*	Transmission rate from $S(t)$ to $SI_b(t)$	ml $Cell^{-1}$ $Year^{-1}$
β_{ab}^*	Transmission rate from $I_a(t)$ to $I_{ab}(t)$	ml $Cell^{-1}$ $Year^{-1}$
β_{ba}^*	Transmission rate from $I_b(t)$ to $I_{ab}(t)$	Km^2 $Vector^{-1}$ $Year^{-1}$
μ	Natural mortality rate of humans	$Year^{-1}$
δ_a^*	Disease induces mortality rate of $I_a(t)$	$Year^{-1}$
δ_b^*	Disease induces mortality rate of $I_b(t)$	$Year^{-1}$
δ_{ab}^*	Disease induces mortality rate of $I_{ab}(t)$	$Year^{-1}$
σ_a^*	Treatment rate of $I_a(t)$	$Year^{-1}$
σ_b^*	Treatment rate of $I_b(t)$	$Year^{-1}$
σ_{ab}^*	Treatment rate of $I_{ab}(t)$	$Year^{-1}$
γ_a^*	Recovery rate of $P_a(t)$ due to treatment	$Year^{-1}$
γ_b^*	Recovery rate of $P_b(t)$ due to treatment	$Year^{-1}$
γ_{ab}^*	Recovery rate of P_{ab} due to treatment	$Year^{-1}$
ω^*	Rate of loss of temporal immunity	$Year^{-1}$
θ_a^*	Rate of treatment failure in $P_a(t)$ due to drug resistance	$Year^{-1}$
θ_b^*	Rate of treatment failure in $P_b(t)$ due to drug resistance	$Year^{-1}$
θ_{ab}^*	Rate of treatment failure in $P_{ab}(t)$ due to drug resistance	$Year^{-1}$
Λ_v^*	Recruitment rate of $X(t)$	Vectors Km^{-2} $Year^{-1}$
α^*	Transmission rate from $Y(t)$ to $S(t)$	Km^2 $Human^{-1}$ $Year^{-1}$
ξ^*	Natural death rate of $X_a(t)$ and $Y_a(t)$	$Year^{-1}$
ϕ^*	Death rate of $X(t)$ and $Y(t)$ due to control intervention	$Year^{-1}$
ν_b^*	Shedding rate of bacteria by $I_b(t)$	Cells Km^2 $Human^{-1}$ ml^{-1} $Year^{-1}$
ν_{ab}^*	Shedding rate of bacteria by $I_{ab}(t)$	Cells Km^2 $Human^{-1}$ ml^{-1} $Year^{-1}$
ρ^*	Natural decay/death rate of bacteria	$Year^{-1}$
ψ^*	Death rate of bacteria due to control interventions	$Year^{-1}$
c_1	Reduction in malaria transmission due to mosquito net	Dimensionless
c_2	Reduction in typhoid fever due to sanitation	Dimensionless

A schematic representation of model (1) is given in the flow diagram below (Figure 1).

To confirm that the malaria and typhoid fever co-infection model (1) is well posed mathematically and epidemiologically, it suffices to establish the positivity and boundedness of solutions of the model. The proofs of the positivity and boundedness of the solutions of the model (1) are presented in Theorems 1 and 2, respectively.

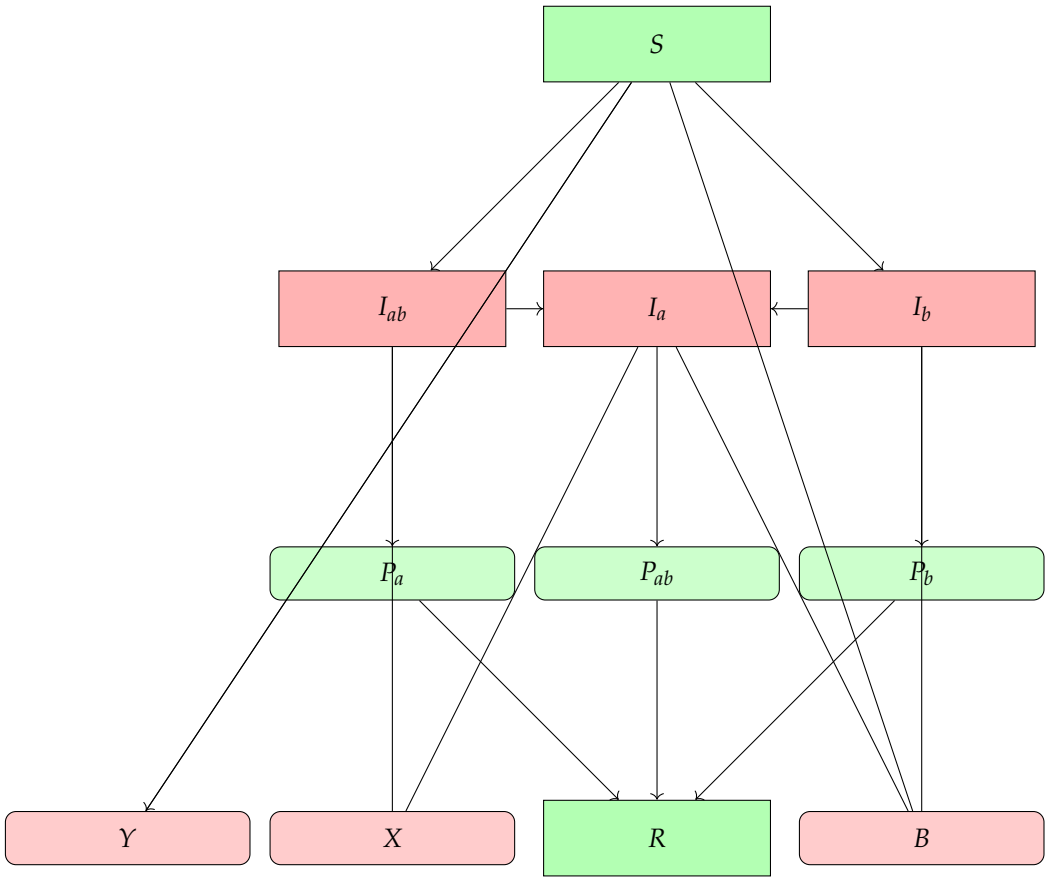


Figure 1. A schematic representation of the malaria and typhoid fever co-infection model (1).

Theorem 1. *Let* $\Omega = \{(S, I_a, I_b, I_{ab}, P_a, P_b, P_{ab}, R, X, Y, B) \in \mathbb{R}^{11}_+ : N_h \leq \frac{\Lambda^*_h}{\mu}, N_v \leq \frac{\Lambda^*_v}{\xi^*}, S(0) \geq 0, I_a(0) \geq 0, I_b(0) \geq 0, I_{ab}(0) \geq 0, P_a(0) \geq 0, P_b(0) \geq 0, P_{ab}(0) \geq 0, R(0) \geq 0, X(0) \geq 0, Y(0) \geq 0, B(0) \geq 0\}$ *then, the solutions* $S(t), I_a(t), I_b(t), I_{ab}(t), P_a(t), P_b(t), P_{ab}(t), R(t), X(t), Y(t), B(t)$ *of the model* (1) *will remain positive for all time* $t > 0$.

Proof. The positivity of solutions of model (1) with initial conditions $S(0) \geq 0$, $I_a(0) \geq 0$, $I_b(0) \geq 0$, $I_{ab}(0) \geq 0$, $P_a(0) \geq 0$, $P_b(0) \geq 0$, $P_{ab}(0) \geq 0, R(0) \geq 0$, $X(0) \geq 0$, $Y(0) \geq 0$ and $B(0) \geq 0$ is established as follows: By rearranging the first equation of model (1), $\frac{dS}{dt} = \Lambda^*_h - (1-c_1)\beta^*_a S(t)Y(t) - (1-c_2)\beta^*_b S(t)B(t) + \omega^* R(t) - \mu S(t)$, we obtain

$$\frac{dS}{dt} + ((1-c_1)\beta^*_a Y + (1-c_2)\beta^*_b B + \mu)S = \Lambda^*_h + \omega^* R. \tag{2}$$

Multiplying Equation (2) by its integrating factor given by $\Psi(t) = e^{\int((1-c_1)\beta^*_a Y + (1-c_2)\beta^*_b B + \mu)dt}$ and simplifying gives

$$\frac{d}{dt}(S(t)\Psi(t)) = (\Lambda^*_h + \omega^* R(t))\Psi(t). \tag{3}$$

Integrating both sides of Equation (3) and simplifying gives

$$S(t)\Psi(t)|^t_0 = \int_0^t (\Lambda^*_h + \omega^* R(t))\Psi(t)dt. \tag{4}$$

Further simplification gives

$$S(t) = \frac{1}{\Psi(t)}\left(S(0) + \int_0^t (\Lambda^*_h + \omega^* R(t))\Psi(t)dt\right). \tag{5}$$

Since $S(0) \geq 0$ and $\Psi(t) = e^{((1-c_1)\beta_a^* Y + (1-c_2)\beta_b^* B + \mu)dt} > 0$, it can be deduced from Equation (5) that $S(t) \geq 0$ for all $t > 0$. Similarly, we can show that $I_a(t), I_b(t), I_{ab}(t), P_a(t), P_b(t), P_{ab}(t), R(t), X(t), Y(t), B(t)$ of the model (1) remain positive for all $t > 0$. □

Theorem 2. *All feasible solutions of the model (1) are bounded in a proper subset* $\Omega = \left\{(S, I_a, I_b, I_{ab}, P_a, P_b, P_{ab}, R, X, Y, B) \in \mathbb{R}_+^{11} : N_h \leq \frac{\Lambda_h^*}{\mu}, N_v \leq \frac{\Lambda_v^*}{\xi^*}, B \leq \frac{(\nu_b^* + \nu_{ab}^*)\Lambda_h^*}{(\rho^* + \psi^*)\mu}\right\}$.

Proof. To establish the boundedness of the solutions of model (1), it suffices to show that a lower bound and upper bound exist for all the solutions of the model. At initial time $t = 0$, $S(0) \geq 0$, $I_a(0) \geq 0$, $I_b(0) \geq 0$, $I_{ab}(0) \geq 0$, $P_a(0) \geq 0$, $P_b(0) \geq 0$, $P_{ab}(0) \geq 0, R(0) \geq 0$, $X(0) \geq 0$, $Y(0) \geq 0$, and $B(0) \geq 0$, establishing the existence of a lower bound.

For the upper bound, we consider the sum of all the equations in model (1) since $N = S + I_a + I_b + I_{ab} + P_a + P_b + P_{ab} + R$ to obtain

$$\frac{dN_h}{dt} = \frac{dS}{dt} + \frac{dI_a}{dt} + \frac{dI_b}{dt} + \frac{dI_{ab}}{dt} + \frac{dP_a}{dt} + \frac{dP_b}{dt} + \frac{dP_{ab}}{dt} + \frac{dR}{dt}. \tag{6}$$

Simplifying Equation (6) gives

$$\frac{dN_h}{dt} = \Lambda_h^* - \mu N_h - \delta_a^* I_a - \delta_b^* I_b - \delta_{ab}^* I_{ab} \leq \Lambda_h^* - \mu N_h. \tag{7}$$

By integrating both sides and applying the initial condition and solving the inequality (7) gives

$$N_h \leq \frac{\Lambda_h^*}{\mu}. \tag{8}$$

Therefore, we obtain

$$0 \leq N_h \leq \frac{\Lambda_h^*}{\mu}. \tag{9}$$

By similar reasoning, we obtain

$$0 \leq N_v \leq \frac{\Lambda_v^*}{\xi^*}. \tag{10}$$

From Equations (1) and (8), we obtain

$$\frac{dB}{dt} = \nu_b^* I_b + \nu_{ab}^* I_{ab} - (\rho^* + \psi^*)B \leq (\nu_b^* + \nu_{ab}^*)\frac{\Lambda_h^*}{\mu} - (\rho^* + \psi^*)B.$$

Similarly, we obtain

$$0 \leq B \leq \frac{(\nu_b^* + \nu_{ab}^*)\Lambda_h^*}{(\rho^* + \psi^*)\mu}. \tag{11}$$

Thus, a feasible solution set of the model enters and remains in the region $\Omega = \left\{(S, I_a, I_b, I_{ab}, P_a, P_b, P_{ab}, R, X, Y, B) \in \mathbb{R}_+^{11} : N_h \leq \frac{\Lambda_h^*}{\mu}, N_v \leq \frac{\Lambda_v^*}{\xi^*}, B \leq \frac{(\nu_b^* + \nu_{ab}^*)\Lambda_h^*}{(\rho^* + \psi^*)\mu}\right\}$. □

3. Analyses and Results

3.1. Model Transformation

The mathematical model (1) comprises the human population, mosquito vector populations, and bacteria in food or water, each having different measurement units. Therefore, to conduct a more accurate analysis of the model, it is crucial to non-dimensionalise it by converting all variables and parameters into dimensionless quantities. This aids in revealing hidden relationships and dependencies between variables and parameters, thereby providing deeper insight into the model dynamics [38,39]. Rescaling model (1) such that $\tau = \mu t$, $s = \frac{S}{N_h^0}$, $i_a = \frac{I_a}{N_h^0}$, $i_b = \frac{I_b}{N_h^0}$, $i_{ab} = \frac{I_{ab}}{N_h^0}$, $p_a = \frac{P_a}{N_h^0}$, $p_b = \frac{P_b}{N_h^0}$, $p_{ab} = \frac{P_{ab}}{N_h^0}$, $r = \frac{R}{N_h^0}$, $x = \frac{X}{N_v^0}$, $y = \frac{Y}{N_v^0}$, $b = \frac{B}{N_b^0}$, $\beta_a = \frac{\beta_a^* N_v^0}{\mu}$, $\beta_b = \frac{\beta_b^* N_b^0}{\mu}$, $\beta_{ab} = \frac{\beta_{ab}^* N_b^0}{\mu}$, $\beta_{ba} =$

$\frac{\beta^*_{ba}N^0_v}{\mu}$, $\sigma_a = \frac{\sigma^*_a}{\mu}$, $\sigma_b = \frac{\sigma^*_b}{\mu}$, $\sigma_{ab} = \frac{\sigma^*_{ab}}{\mu}$, $\delta = \frac{\delta^*_a}{\mu}$, $\delta_b = \frac{\delta^*_b}{\mu}$, $\delta_{ab} = \frac{\delta^*_{ab}}{\mu}$, $\theta_a = \frac{\theta^*_a}{\mu}$, $\theta_b = \frac{\theta^*_b}{\mu}$, $\theta_{ab} = \frac{\theta^*_{ab}}{\mu}$, $\gamma = \frac{\gamma^*_a}{\mu}$, $\gamma_b = \frac{\gamma^*_b}{\mu}$, $\gamma_{ab} = \frac{\gamma^*_{ab}}{\mu}$, $\omega = \frac{\omega^*}{\mu}$, $\alpha = \frac{\alpha^* N^0_h}{\mu}$, $\xi = \frac{\xi^*}{\mu}$, $\phi = \frac{\phi^*}{\mu}$, $\rho = \frac{\rho^*}{\mu}$, $\psi = \frac{\psi^*}{\mu}$, $\nu_b = \frac{\nu^*_b N^0_h}{\mu N^0_b}$, $\nu_{ab} = \frac{\nu^*_{ab} N^0_h}{\mu N^0_b}$, $N^0_h = S(0) + I_a(0) + I_b(0) + I_{ab}(0) + P_a(0) + P_b(0) + P_{ab}(0) + R(0)$, $N^0_v = X(0) + Y(0)$, $N^0_b = B(0)$, and if $\Lambda^*_h = \mu N^0_v$, $\Lambda^*_v = \mu N^0_v$, the dimensionless version of model (1) is obtained as follows:

$$
\begin{aligned}
\frac{ds(\tau)}{d\tau} &= 1 - (1-c_1)\beta_a s(\tau)y(\tau) - (1-c_2)\beta_b s(\tau)b(\tau) + \omega r(\tau) - s(\tau),\\
\frac{di_a(\tau)}{d\tau} &= (1-c_1)\beta_a s(\tau)y(\tau) + \theta_a p_a(\tau) - (1-c_2)\beta_{ab} i_a(\tau)b(\tau) - (1+\sigma_a+\delta_a)i_a(\tau),\\
\frac{di_b(\tau)}{d\tau} &= (1-c_2)\beta_b s(\tau)b(\tau) + \theta_b p_b(\tau) - (1-c_1)\beta_{ba} i_b(\tau)y(\tau) - (1+\sigma_b+\delta_b)i_b(\tau),\\
\frac{di_{ab}(\tau)}{d\tau} &= (1-c_2)\beta_{ab} i_a(\tau)b(\tau) + (1-c_1)\beta_{ba} i_b(\tau)y(\tau) + \theta_{ab} p_{ab}(\tau) - (1+\sigma_{ab}+\delta_{ab})i_{ab}(\tau),\\
\frac{dp_a(\tau)}{d\tau} &= \sigma_a i_a(\tau) - (1+\gamma_a+\theta_a)p_a(\tau),\\
\frac{dp_b(\tau)}{d\tau} &= \sigma_b i_b(\tau) - (1+\gamma_b+\theta_b)p_b(\tau),\\
\frac{dp_{ab}(\tau)}{d\tau} &= \sigma_{ab} i_{ab}(\tau) - (1+\gamma_{ab}+\theta_{ab})p_{ab}(\tau),\\
\frac{dr(\tau)}{d\tau} &= \gamma_a p_a(\tau) + \gamma_b p_b(\tau) + \gamma_{ab} p_{ab}(\tau) - (1+\omega)r(\tau),\\
\frac{dx(\tau)}{d\tau} &= 1 - (1-c_1)\alpha x(\tau)(i_a(\tau) + i_{ab}(\tau)) - (\xi+\phi)x(\tau),\\
\frac{dy(\tau)}{d\tau} &= (1-c_1)\alpha x(\tau)(i_a(\tau) + i_{ab}(\tau)) - (\xi+\phi)y(\tau),\\
\frac{db(\tau)}{d\tau} &= \nu_b i_b(\tau) + \nu_{ab} i_{ab}(\tau) - (\rho+\psi)b(\tau).
\end{aligned}
\tag{12}
$$

The following assumptions are introduced for simplicity where appropriate: $k_1 = (1-c_1)\beta_a$, $k_2 = 1+\sigma_a+\delta_a$, $k_3 = 1+\gamma_a+\theta_a$, $k_4 = 1+\omega$, $k_5 = (1-c_1)\alpha$, $k_6 = \xi+\phi$, $l_1 = (1-c_2)\beta_b$, $l_2 = 1+\sigma_b+\delta_b$, $l_3 = 1+\gamma_b+\theta_b$, $l_4 = 1+\omega$, $l_5 = \rho+\psi$, $d_1 = (1-c_2)\beta_{ab}$, $d_2 = (1-c_1)\beta_{ba}$, $d_3 = 1+\sigma_{ab}+\delta_{ab}$, $d_4 = 1+\gamma_{ab}+\theta_{ab}$.

3.2. Malaria Sub-Model and Analysis

The malaria sub-model is a special case of the co-infection model (12) where malaria is the only disease affecting the population. Dynamical system analysis of this special case, essential for understanding the transmission dynamics and control interventions of malaria, is presented in this section. The malaria sub-model is obtained by setting $i_b(\tau) = i_{ab}(\tau) = p_b(\tau) = p_{ab}(\tau) = b(\tau) = 0$ in the model (12), to obtain

$$
\begin{aligned}
\frac{ds(\tau)}{d\tau} &= 1 - k_1 s(\tau)y(\tau) + \omega r(\tau) - s(\tau),\\
\frac{di_a(\tau)}{d\tau} &= k_1 s(\tau)y(\tau) + \theta_a p_a(\tau) - k_2 i_a(\tau),\\
\frac{dp_a(\tau)}{d\tau} &= \sigma_a i_a(\tau) - k_3 p_a(\tau),\\
\frac{dr(\tau)}{d\tau} &= \gamma_a p_a(\tau) - k_4 r(\tau),\\
\frac{dx(\tau)}{d\tau} &= 1 - k_5 x(\tau) i_a(\tau) - k_6 x(\tau),\\
\frac{dy(\tau)}{d\tau} &= k_5 x(\tau) i_a(\tau) - k_6 y(\tau),
\end{aligned}
\tag{13}
$$

where $k_1 = (1-c_1)\beta_a$, $k_2 = 1+\sigma_a+\delta_a$, $k_3 = 1+\gamma_a+\theta_a$, $k_4 = 1+\omega$, $k_5 = (1-c_1)\alpha$, $k_6 = \xi+\phi$ are assumed to simplify the analysis. An analysis of sub-model (13) that reveals the qualitative dynamics and impact of control interventions for a malaria disease outbreak is presented in this section.

3.2.1. Equilibrium Points of the Malaria Sub-Model (13)

Most mathematical epidemiological models have two important equilibrium points, namely, the disease-free equilibrium (DFE) and the endemic equilibrium (EE) [4,5]. The DFE is the equilibrium point of the model when there is no disease in the system, while the EE is the equilibrium point of the model when there is disease in the system. The analytical representation of the DFE of the malaria sub-model (13) is given by

$$(s^0,\ i_a^0,\ p_a^0,\ r^0,\ x^0,\ y^0) = \left(1,\ 0,\ 0,\ 0,\ \frac{1}{k_6},\ 0\right). \tag{14}$$

For simplicity in the determination of the endemic equilibrium (EE), we assume that $\delta_a = 0$ and $k_6 = 1$. Based on these assumptions, we have $x^* + y^* = 1$ and $s^* + i_a^* + p_a^* + r^* = 1$. Using these assumptions for $\mathcal{R}_0^a > 1$, there exists an EE of the malaria sub-model (13) given by

$$(s^*,\ i_a^*,\ p_a^*,\ r^*,\ x^*,\ y^*) = \left(\frac{B_3 i_a^{*2} + B_4 i_a^* + 1}{B_5 i_a^* + 1},\ i_a^*,\ B_1 i_a^*,\ B_2 i_a^*,\ 1-y^*,\ \frac{k_5 i_a^*}{1+k_5 i_a^*}\right), \tag{15}$$

where $i_a^* = \frac{B_5 - B_4 - B_6}{B_3 + B_6 B_5}$, $B_1 = \frac{\sigma_a}{k_3}$, $B_2 = \frac{\gamma_a \sigma_a}{k_3 k_4}$, $B_3 = \omega k_5 B_2$, $B_4 = k_5 + \omega B_2$, $B_5 = k_5(1+k_1)$ provided $B_5 - B_4 - B_6 > 0$.

Due to the complexity of the equations involved, the transmission dynamics of the malaria sub-model (13) about the EE will be explored numerically.

3.2.2. The Basic Reproduction Number of the Malaria Sub-Model (13)

The basic reproduction number of an epidemiological model represents the average number of infectious cases generated by one case in a population where all individuals are susceptible to the infection [4,5]. The value of the basic reproduction number indicates whether an outbreak will be eradicated or persist [4,5]. The basic reproduction number for the malaria sub-model (13) denoted by $\mathcal{R}_0^a$ is determined using the next-generation matrix method [4]. The next-generation matrix of the malaria sub-model (13) is computed as

$$FV^{-1} = \begin{pmatrix} 0 & 0 & \frac{k_1}{k_6} \\ 0 & 0 & 0 \\ \frac{k_5 k_3 x^0}{k_2 k_3 - \theta_a \sigma_a} & \frac{k_5 \theta_a x^0}{k_2 k_3 - \theta_a \sigma_a} & 0 \end{pmatrix}, \tag{16}$$

where

$$F = \begin{pmatrix} 0 & 0 & k_1 \\ 0 & 0 & 0 \\ k_5 x^0 & 0 & 0 \end{pmatrix} \quad \text{and} \quad V = \begin{pmatrix} k_2 & -\theta_a & 0 \\ -\sigma_a & k_3 & 0 \\ 0 & 0 & k_6 \end{pmatrix}.$$

The $\mathcal{R}_0^a$ associated with the malaria sub-model (13) is calculated as the dominant eigenvalue of the next-generation matrix FV^{-1} and is

$$\mathcal{R}_0^a = \sqrt{\frac{k_1 k_3 k_5 x^0}{k_6(k_2 k_3 - \theta_a \sigma_a)}}, \tag{17}$$

which can be re-written explicitly as

$$(\mathcal{R}_0^a)^2 = \frac{k_1 k_3 k_5 x^0}{k_6(k_2 k_3 - \theta_a \sigma_a)}, \tag{18}$$

where $k_2 k_3 - \theta_a \sigma_a = \sigma_a(1+\gamma_a) + (1+\delta_1)k_3 > 0$.

3.2.3. Stability Analysis of the Malaria Sub-Model (13)

The stability analysis of an epidemiological model about its equilibrium point describes the dynamics of the model about the equilibrium point. The results of the stability analysis of the malaria sub-model (13) are summarised in the subsequent theorems.

Theorem 3. *The malaria sub-model* (13) *is globally asymptotically stable about the DFE* (14) *provided* $\mathcal{R}_0^a < 1$.

The proof of Theorem 3 will be established using a stability result in [40], which is stated in Lemma 1.

Lemma 1 ([40])**.** *Consider a model system written in the form*

$$\begin{aligned} \frac{dZ_1}{dt} &= F(Z_1, Z_2) \\ \frac{dZ_2}{dt} &= G(Z_1, Z_2), \quad G(Z_1, 0) = 0, \end{aligned} \tag{19}$$

where $Z_1 \in R^m$ *and* $Z_2 \in R^n$. $Z_0 = (Z_1^*, 0)$ *denotes the disease-free equilibrium of the system. Assume that*

(H1) For $\frac{dZ_1}{dt} = F(Z_1, 0)$, Z_1^* *is globally asymptotically stable;*

(H2) $G(Z_1, Z_2) = AZ_2 - \hat{G}(Z_1, Z_2)$, $\hat{G}(Z_1, Z_2) \geq 0$ *for* $(Z_1, Z_2) \in \Omega$, *where the Jacobian* $A = \frac{\partial G}{\partial Z_2}(Z_1, 0)$ *is an M–matrix (the off-diagonal elements of A are non-negative) and* Ω *is the region where the model makes biological sense.*

Then, the disease-free equilibrium Z_0 *is globally asymptotically stable provided that the basic reproduction number is less than one [40].*

Proof. To consider Lemma 1, it suffices to show that conditions H1 and H2 of the Lemma are satisfied. From the malaria sub-model Equation (13), let $Z_1 = (s, r, x)$, $Z_2 = (i_a, p_a, y)$. So, the disease-free part of the model (13) is

$$\frac{dZ_1}{d\tau} = F(Z_1, 0) = \begin{pmatrix} \frac{ds(\tau)}{d\tau} \\ \frac{dr(\tau)}{d\tau} \\ \frac{dx(\tau)}{d\tau} \end{pmatrix} = \begin{pmatrix} 1 + \omega r(\tau) - s(\tau) \\ -k_4 r(\tau) \\ 1 - k_5 x(\tau) \end{pmatrix}, \tag{20}$$

whereas the disease part of the model (13) is

$$\frac{dZ_2}{d\tau} = G(Z_1, Z_2) = \begin{pmatrix} k_1 s(\tau) y(\tau) + \theta_a p_a(\tau) - k_2 i_a(\tau) \\ \sigma_a i_a(\tau) - k_3 p_a(\tau) \\ k_5 x(\tau) i_a(\tau) - k_6 y(\tau) \end{pmatrix}. \tag{21}$$

The disease-free part (20) consists of a set of linear ordinary differential equations and its exact solution can be obtained as $s(\tau) = 1 + \frac{\omega B_1 e^{-k_4 \tau}}{1-k_4} + B_2 e^{-\tau}$, $r(\tau) = B_1 e^{-k_4 \tau}$, $x(\tau) = \frac{1}{k_6} + B_3 e^{-k_6 \tau}$, where B_1, B_2, B_3 are constants of integration. As $\tau \longrightarrow \infty$, $s(\tau) \longrightarrow s^0 = 1$, $r(\tau) \longrightarrow r^0 = 0$ and $x(\tau) \longrightarrow x^0 = \frac{1}{k_6}$. This shows that the disease-free part of model (13) is globally asymptotically stable, confirming condition H1 of Lemma 1.

For the disease part, the Jacobian of the malaria sub-model (13) about the disease-free equilibrium is determined as

$$A = \begin{pmatrix} -k_2 & \theta_a & k_1 s^0 \\ \sigma_a & -k_3 & 0 \\ k_5 x^0 & 0 & -k_6 \end{pmatrix}, \tag{22}$$

where A is an M–matrix with all its off-diagonal elements non-negative. From Equations (21) and (22), the term $\hat{G}(Z_1, Z_2)$ is determined as

$$\hat{G}(Z_1, Z_2) = \begin{pmatrix} k_1 y(s^0 - s) \\ 0 \\ k_5 i_a (x^0 - x) \end{pmatrix}. \tag{23}$$

Clearly, $\hat{G}(Z_1, Z_2) \geq 0$, since $s^0 \geq s$ and $x^0 \geq x$, confirming that condition (H_2) holds and thus the proof is complete. □

The epidemiological implication of this result is that the malaria disease outbreak could be eradicated irrespective of the sizes of the infected human population and the mosquito vectors at the initial stage of the outbreak, provided the control interventions are effective enough to keep $\mathcal{R}_0^a$ below unity.

3.3. Typhoid Fever Sub-Model and Analysis

The typhoid fever sub-model is a special case of the co-infection model (12) where typhoid fever is the only disease affecting the population. Qualitative analysis of this special case is crucial for understanding the transmission dynamics and control intervention of typhoid fever and is presented in this section. The typhoid fever sub-model is obtained by setting $i_a = i_{ab} = p_a = p_{ab} = x = y = 0$ in the model (12), to obtain

$$\begin{aligned} \frac{ds(\tau)}{d\tau} &= 1 - l_1 s(\tau) b(\tau) + \omega r(\tau) - s(\tau), \\ \frac{di_b(\tau)}{d\tau} &= l_1 s(\tau) b(\tau) + \theta_b p_b(\tau) - l_2 i_b(\tau), \\ \frac{dp_b(\tau)}{d\tau} &= \sigma_b i_b(\tau) - l_3 p_b(\tau), \\ \frac{dr(\tau)}{d\tau} &= \gamma_b p_b(\tau) - l_4 r(\tau), \\ \frac{db(\tau)}{d\tau} &= \nu_b i_b(\tau) - l_5 b(\tau), \end{aligned} \tag{24}$$

where $l_1 = (1 - c_2)\beta_b$, $l_2 = 1 + \sigma_b + \delta_b$, $l_3 = 1 + \gamma_b + \theta_b$, $l_4 = 1 + \omega$, $l_5 = \rho + \psi$. The analysis of sub-model (24), which is essential for understanding the dynamics and the impact of control interventions of typhoid fever transmissions, is presented in this section

3.3.1. Equilibrium Points of Typhoid Fever Sub-Model (24)

The analytical representation of the DFE of the typhoid fever sub-model (24) is given by

$$(s^0,\ i_b^0,\ p_b^0,\ r^0,\ b^0) = (1,\ 0,\ 0,\ 0,\ 0). \tag{25}$$

For $\mathcal{R}_0^b > 1$, the typhoid fever sub-model (24) has an endemic equilibrium which is represented analytically by

$$(s^*,\ i_b^*,\ p_b^*,\ r^*,\ b^*) = \left(\frac{1 + \omega D_3 i_b^*}{1 + l_1 D_1 i_b^*},\ \frac{D_5}{D_6},\ D_2 i_b^*,\ D_3 i_b^*,\ D_1 i_b^* \right), \tag{26}$$

where $D_1 = \frac{\nu_b}{l_5}$, $D_2 = \frac{\sigma_b}{l_3}$, $D_3 = \frac{\gamma_b \sigma_b}{l_3 l_4}$, $D_4 = l_2 - \theta_b D_2$, $D_5 = D_4 - l_1 D_1$, $D_6 = l_1 D_1 (D_3 \omega - D_4)$. Due to the complexity of the equations involved in the analytical representation of the model dynamics about the EE of the typhoid fever sub-model (24), the stability analysis about the EE of the typhoid fever sub-model (24) will be explored numerically.

3.3.2. The Basic Reproduction Number of the Typhoid Fever Sub-Model (24)

The basic reproduction number of the typhoid fever sub-model (24), denoted by $\mathcal{R}_0^b$, is computed using the next-generation matrix method [4]. The next-generation matrix of the typhoid fever sub-model (24) is

$$FV^{-1} = \begin{pmatrix} \frac{l_1 s^0 l_3 \nu_b}{l_5(l_2 l_3 - \theta_b \sigma_b)} & \frac{l_1 s^0 \theta_b \nu_b}{l_5(l_2 l_3 - \theta_b \sigma_b)} & \frac{l_1 s^0}{l_5} \\ 0 & 0 & 0 \\ 0 & 0 & 0 \end{pmatrix}, \tag{27}$$

where

$$F = \begin{pmatrix} 0 & 0 & l_1 s^0 \\ 0 & 0 & 0 \\ 0 & 0 & 0 \end{pmatrix} \quad \text{and} \quad V = \begin{pmatrix} l_2 & -\theta_b & 0 \\ -\sigma_b & l_3 & 0 \\ -\nu_b & 0 & l_5 \end{pmatrix}.$$

The dominant eigenvalue of the next-generation matrix FV^{-1} is the $\mathcal{R}_0^b$ and is determined as

$$\mathcal{R}_0^b = \frac{l_1 l_3 \nu_b}{l_5(l_2 l_3 - \theta_b \sigma_b)}, \tag{28}$$

where $l_2 l_3 - \theta_b \sigma_b = \sigma_b(1 + \gamma_b) + (1 + \delta_b) l_3 > 0$.

3.3.3. Stability Analysis of the Typhoid Fever Sub-Model (24)

The stability analysis of the typhoid fever sub-model (24) about the DFE (25) is summarised in the following theorems.

Theorem 4. *The typhoid fever sub-model (24) is globally asymptotically stable about the DFE (25) provided* $\mathcal{R}_0^b < 1$.

The proof of Theorem 3 will be established using a stability result in [40], which is stated in Lemma 1.

Proof. To apply Lemma 1, it suffices to show that the disease-free part of model (24) is globally stable (condition (H1)) and the disease part of model (24) satisfies conditions H2 of the Lemma. From the typhoid fever sub-model Equation (24), let $Z_1 = (s, r)$, $Z_2 = (i_b, p_b, b)$. So, the disease-free part of model (24) is given by

$$\frac{dZ_1}{d\tau} = F(Z_1, 0) = \begin{pmatrix} \frac{ds(\tau)}{d\tau} \\ \frac{dr(\tau)}{d\tau} \end{pmatrix} = \begin{pmatrix} 1 + \omega r(\tau) - s(\tau) \\ -l_4 r(\tau) \end{pmatrix}, \tag{29}$$

while the disease part of model (24) is

$$\frac{dZ_2}{d\tau} = G(Z_1, Z_2) = \begin{pmatrix} l_1 s(\tau) b(\tau) + \theta_b p_b(\tau) - l_2 i_b(\tau) \\ \sigma_b i_b(\tau) - l_3 p_b(\tau) \\ \nu_b i_b(\tau) - l_5 b(\tau) \end{pmatrix}. \tag{30}$$

The disease-free part (29) consists of a set of linear ordinary differential equations and its exact solution can be obtained as $s(\tau) = 1 + \frac{\omega D_1 e^{-l_4 \tau}}{1 - l_4} + D_2 e^{-\tau}$, $r(\tau) = D_1 e^{-l_4 \tau}$, where

D_1, D_2 are constants of integration. As $\tau \longrightarrow \infty, s(\tau) \longrightarrow s^0 = 1, r(\tau) \longrightarrow r^0 = 0$. This shows that the disease-free part of model (24) is globally asymptotically stable, confirming condition H1 of Lemma 1.

For the disease part, the Jacobian of (21) about the disease-free equilibrium is determined as

$$A = \begin{pmatrix} -l_2 & \theta_b & l_1 s^0 \\ \sigma_b & -l_3 & 0 \\ \nu_b & 0 & -l_5 \end{pmatrix}, \tag{31}$$

where A is an M–matrix with all its off-diagonal elements non-negative. From Equations (30) and (31), the term $\hat{G}(Z_1, Z_2)$ is determined as

$$\hat{G}(Z_1, Z_2) = \begin{pmatrix} l_1 b(s^0 - s) \\ 0 \\ 0 \end{pmatrix}. \tag{32}$$

Clearly, $\hat{G}(Z_1, Z_2) \geq 0$, since $s^0 \geq s$, confirming that condition (H_2) holds and thus the proof is complete. □

The epidemiological implication of this result is that the typhoid fever disease outbreak could be eradicated irrespective of the size of the infected population at the initial stage of the outbreak, provided the control interventions are effective enough to keep $\mathcal{R}_0^b$ below unity.

3.4. Analysis of the Malaria and Typhoid Fever Co-Infection Model (12)

The dynamical system analysis of the malaria and typhoid fever co-infection model (12) is presented in this section. This analysis is crucial for understanding the transmission dynamics and the impact of the control interventions on malaria and typhoid fever co-infection.

3.4.1. Equilibrium Points of the Malaria and Typhoid Fever Co-Infection Model (12)

The malaria and typhoid fever co-infection model (12) has several equilibrium points. The analytical representation of the disease-free equilibrium points (DFE) of the malaria and typhoid fever co-infection model (12) is given by

$$(s^0,\ i_a^0,\ i_b^0,\ i_{ab}^0,\ p_a^0,\ p_b^0,\ p_{ab}^0,\ r^0,\ x^0,\ y^0,\ b^0) = \left(1,\ 0,\ 0,\ 0,\ 0,\ 0,\ 0,\ 0,\ \frac{1}{k_5},\ 0,\ 0\right). \tag{33}$$

The analytical representation of the EE of the malaria and typhoid fever co-infection model (12) is complex, so it will be explored numerically.

The malaria and typhoid fever co-infection model (12) has a malaria-only equilibrium point. This is an equilibrium point where malaria is the only infection in the system. To determine this equilibrium point, we make the following assumptions to simplify the analysis: $\delta_a = 0$ and $k_6 = 1$. Based on these assumptions, we have $x^* + y^* = 1$ and $s^* + i_a^* + p_a^* + r^* = 1$. Using these assumptions and for $\mathcal{R}_0 > 1$, there exists a malaria-only EE of the malaria and typhoid fever co-infection model (12) given by

$$(s^*,\ i_a^*,\ i_b^*,\ i_{ab}^*,\ p_a^*,\ p_b^*,\ p_{ab}^*,\ r^*,\ x^*,\ y^*,\ b^*) = (s^*,\ \ i_a^*,\ 0,\ 0,\ B_1 i_a^*,\ 0,\ 0,\ B_2 i_a^*,\ \ 1 - y^*,\ y^*, 0), \tag{34}$$

where $s^* = \frac{B_3 i_a^{*2} + B_4 i_a^* + 1}{B_5 i_a^* + 1}$, $y^* = \frac{k_5 i_a^*}{1 + k_5 i_a^*}$, $i_a^* = \frac{B_5 - B_4 - B_6}{B_3 + B_6 B_5}$, $B_1 = \frac{\sigma_a}{k_3}$, $B_2 = \frac{\gamma_a \sigma_a}{k_3 k_4}$, $B_3 = \omega k_5 B_2$, $B_4 = k_5 + \omega B_2$, $B_5 = k_5(1 + k_1)$ provided $B_5 - B_4 - B_6 > 0$. Due to the complexity of the equations involved, the transmission dynamics of the malaria and typhoid fever co-infection model (12) about the malaria-only EE will be explored numerically.

Furthermore, the malaria and typhoid fever co-infection model (12) has a typhoid-fever-only equilibrium point. This is an equilibrium point where typhoid fever is the only infection in the system. For $\mathcal{R}_0 > 1$, there exists a typhoid-fever-only EE of the malaria and typhoid fever co-infection model (12) given by

$$(s^*, i_a^*, i_b^*, i_{ab}^*, p_a^*, p_b^*, p_{ab}^*, r^*, x^*, y^*, b^*) = \left(s^*, 0, \frac{D_5}{D_6}, 0, 0, D_2 i_b^*, 0, D_3 i_b^*, \frac{1}{K_5}, 0, D_1 i_b^*\right), \tag{35}$$

where $s^* = \frac{1+\omega D_3 i_b^*}{1+l_1 D_1 i_b^*}$, $D_1 = \frac{\nu_b}{l_5}$, $D_2 = \frac{\sigma_b}{l_3}$, $D_3 = \frac{\gamma_b \sigma_b}{l_3 l_4}$, $D_4 = l_2 - \theta_b D_2$, $D_5 = D_4 - l_1 D_1$, $D_6 = l_1 D_1 (D_3 \omega - D_4)$. Due to the complexity of the equations involved, the transmission dynamics of the malaria and typhoid fever co-infection model (12) about the typhoid-fever-only EE will be explored numerically.

3.4.2. Basic Reproduction Number of the Malaria and Typhoid Fever Co-Infection Model (12)

The basic reproduction number of the malaria and typhoid fever co-infection model (12) denoted by $\mathcal{R}_0$ is computed using the next-generation matrix method [4]. The next-generation matrix of the malaria and typhoid fever co-infection model (12) is

$$FV^{-1} = \begin{pmatrix} 0 & 0 & 0 & 0 & 0 & 0 & \frac{k_1}{k_6} & 0 \\ 0 & \frac{l_1 l_3 \nu_b}{l_5(l_2 l_3 - \theta_b \sigma_b)} & \frac{l_1 d_4 \nu_{ab}}{l_5(d_3 d_4 - \theta_{ab}\sigma_{ab})} & 0 & \frac{l_1 \theta_b \nu_b}{l_5(l_2 l_3 - \theta_b \sigma_b)} & \frac{l_1 \theta_{ab} \nu_{ab}}{l_5(d_3 d_4 - \theta_{ab}\sigma_{ab})} & 0 & \frac{l_1}{l_5} \\ 0 & 0 & 0 & 0 & 0 & 0 & 0 & 0 \\ 0 & 0 & 0 & 0 & 0 & 0 & 0 & 0 \\ 0 & 0 & 0 & 0 & 0 & 0 & 0 & 0 \\ 0 & 0 & 0 & 0 & 0 & 0 & 0 & 0 \\ \frac{k_3 k_5 x^0}{k_2 k_3 - \theta_a \sigma_a} & 0 & \frac{d_4 k_5 x^0}{d_3 d_4 - \theta_{ab}\sigma_{ab}} & \frac{\theta_a k_5 x^0}{k_2 k_3 - \theta_a \sigma_a} & 0 & \frac{\theta_{ab} k_5 x^0}{d_3 d_4 - \theta_{ab}\sigma_{ab}} & 0 & 0 \\ 0 & 0 & 0 & 0 & 0 & 0 & 0 & 0 \end{pmatrix}, \tag{36}$$

where

$$F = \begin{pmatrix} 0 & 0 & 0 & 0 & 0 & 0 & k_1 & 0 \\ 0 & 0 & 0 & 0 & 0 & 0 & 0 & l_1 \\ 0 & 0 & 0 & 0 & 0 & 0 & 0 & 0 \\ 0 & 0 & 0 & 0 & 0 & 0 & 0 & 0 \\ 0 & 0 & 0 & 0 & 0 & 0 & 0 & 0 \\ 0 & 0 & 0 & 0 & 0 & 0 & 0 & 0 \\ k_5 x^0 & 0 & k_5 x^0 & 0 & 0 & 0 & 0 & 0 \\ 0 & 0 & 0 & 0 & 0 & 0 & 0 & 0 \end{pmatrix}$$

and

$$V = \begin{pmatrix} k_2 & 0 & 0 & -\theta_a & 0 & 0 & 0 & 0 \\ 0 & l_2 & 0 & 0 & -\theta_b & 0 & 0 & 0 \\ 0 & 0 & d_3 & 0 & 0 & -\theta_{ab} & 0 & 0 \\ -\sigma_a & 0 & 0 & k_3 & 0 & 0 & 0 & 0 \\ 0 & -\sigma_b & 0 & 0 & l_3 & 0 & 0 & 0 \\ 0 & 0 & -\sigma_{ab} & 0 & 0 & d_4 & 0 & 0 \\ 0 & 0 & 0 & 0 & 0 & 0 & k_6 & 0 \\ 0 & -\nu_b & -\nu_{ab} & 0 & 0 & 0 & 0 & l_5 \end{pmatrix}.$$

The dominant eigenvalue of the next-generation matrix FV^{-1} is the $\mathcal{R}_0$ and is obtained as

$$\mathcal{R}_0 = \max\{\mathcal{R}_0^a,\ \mathcal{R}_0^b\}, \tag{37}$$

where

$$\mathcal{R}_0^a = \sqrt{\frac{k_1 k_3 k_5 x^0}{k_6(k_2 k_3 - \theta_a \sigma_a)}},\quad \mathcal{R}_0^b = \frac{l_1 l_3 \nu_b}{l_5(l_2 l_3 - \theta_b \sigma_b)}. \tag{38}$$

This shows that $\mathcal{R}_0$ of the full co-infection model is the maximum of the individual typhoid fever and malaria. Epidemiologically, an increase in the basic reproduction number implies an increase in the spread of infection. Hence, co-infection by malaria and typhoid fever might lead to a greater spread of infections.

3.4.3. Stability Analysis of the Malaria and Typhoid Fever Co-Infection Model (12)

The result of the stability analysis of the malaria and typhoid fever co-infection model (12) is summarised in the theorem below.

Theorem 5. *For $\mathcal{R}_0 < 1$, the malaria and typhoid fever co-infection model (12) is not globally asymptotically stable about the DFE (33).*

The proof of Theorem 5 is established using Lemma 1.

Proof. To prove Theorem 5 using Lemma 1, it is sufficient to show that the model fails to satisfy one of the conditions of the global stability conditions of Lemma 1 [40]. From the malaria and typhoid fever co-infection model (12), let $Z_1 = (s, r, x)$, $Z_2 = (i_a, i_b, i_{ab}, p_a, p_b, p_{ab}, y, b)$. So, the disease-free part of the malaria and typhoid fever co-infection model (12) is given by

$$\frac{dZ_1}{d\tau} = F(Z_1, 0) = \begin{pmatrix} 1 + \omega r(\tau) - s(\tau) \\ -k_4 r(\tau) \\ 1 - k_5 x(\tau) \end{pmatrix} \tag{39}$$

whereas the disease part of the malaria–typhoid fever co-infection model (12) is

$$\frac{dZ_2}{d\tau} = G(Z_1, Z_2) = \begin{pmatrix} k_1 s(\tau) y(\tau) + \theta_a p_a(\tau) - d_1 i_a(\tau) b(\tau) - k_2 i_a(\tau) \\ l_1 s(\tau) b(\tau) + \theta_b p_b(\tau) - d_2 i_b(\tau) y(\tau) - l_2 i_b(\tau) \\ d_1 i_a(\tau) b(\tau) + d_2 i_b(\tau) y(\tau) + \theta_{ab} p_{ab}(\tau) - d_3 i_{ab}(\tau) \\ \sigma_a i_a(\tau) - k_3 p_a(\tau) \\ \sigma_b i_b(\tau) - l_3 p_b(\tau) \\ \sigma_{ab} i_{ab}(\tau) - d_4 p_{ab}(\tau) \\ k_5 x(\tau)(i_a(\tau) + i_{ab}(\tau)) - k_6 y(\tau) \\ \nu_b i_b(\tau) + \nu_{ab} i_{ab}(\tau) - l_5 b(\tau). \end{pmatrix}. \tag{40}$$

The Jacobian of the disease part (40) about the disease-free equilibrium is

$$A = \begin{pmatrix} k_2 & 0 & 0 & \theta_a & 0 & 0 & k_1 & 0 \\ 0 & l_2 & 0 & 0 & \theta_b & 0 & 0 & l_1 \\ 0 & 0 & d_3 & 0 & 0 & \theta_{ab} & k_1 & 0 \\ \sigma_a & 0 & 0 & -k_3 & 0 & 0 & 0 & 0 \\ 0 & \sigma_b & 0 & 0 & -l_3 & 0 & 0 & 0 \\ 0 & 0 & \sigma_{ab} & 0 & 0 & -d_4 & 0 & 0 \\ k_5 x^0 & 0 & k_5 x^0 & 0 & 0 & 0 & -k_6 & 0 \\ 0 & \nu_b & \nu_{ab} & 0 & 0 & 0 & 0 & -l_5 \end{pmatrix}, \tag{41}$$

where A is an M–matrix with all its off-diagonal elements non-negative. From Equations (40) and (41), the expression $\hat{G}(Z_1, Z_2)$ is calculated as

$$\hat{G}(Z_1, Z_2) = \begin{pmatrix} k_1 y(s^0 - s) + d_1 i_a b \\ l_1 b(s^0 - s) + d_2 i_b y \\ -d_1 i_a b - d_2 i_b y \\ 0 \\ 0 \\ 0 \\ k_5(i_a + i_{ab})x^0 - x) \\ 0 \end{pmatrix}. \tag{42}$$

Clearly, $\hat{G}(Z_1, Z_2)$ is not positive, showing that condition (H_2) does not hold and hence completes the proof. □

The implication of these results is that it will be difficult to eradicate malaria and typhoid fever co-infection simultaneously by only lowering $\mathcal{R}_0$ below unity. This could explain why malaria and typhoid fever co-infection is more severe and difficult to eradicate.

4. Numerical Simulations

In this section, numerical simulations are considered to explore the transmission dynamics and impact of control interventions on the malaria and typhoid fever co-infection model (12) using Nigeria as a case study. Malaria and typhoid fever including their co-infection cases have been endemic in Nigeria for a long period [41,42]. Insights gained from this study can inform broader strategies aimed at combating malaria and typhoid fever outbreaks in the endemic areas.

4.1. Model Fitting, Model Prediction, and Parameter Estimation

Malaria and typhoid fever have been endemic in Nigeria for many years, so fitting the model (12) to malaria data will be helpful in making future predictions of the malaria disease dynamics. The incidence of malaria in Nigeria from 2000 to 2023 extracted from [43] is used in this study. Unfortunately, real data on the incidence of typhoid fever in Nigeria from 2000 to 2023 were not available at the time of this study. So, model (12) is fitted and some important parameters are estimated using data for the incidence of malaria in Nigeria from 2000 to 2023. The estimated parameter values together with other parameter values used for the numerical simulations with their sources are given in Table 3.

Model (12) is non-dimensionalised; therefore, to fit the model to the data, the incidence is converted to fractions by dividing it by 1000. The irregular fluctuation over years in the data is taken into consideration by multiplying the transmission rates β_a and β_b by a function $(1 + 0.1\sin(\frac{\pi t}{4}) + 0.3\sin(\frac{\pi t}{12}))$, where t is given by years [8,15]. The parameter value units in Table 3 that are per day are converted to per year to match the time-scale of the data.

Table 3. Parameter values used in the simulation.

Parameter	Value	References
β_a	7.9970	Estimated
β_b	2.5162	Estimated
β_{ab}	0.2 β_a	Estimated
β_{ba}	0.2 β_b	Estimated
ω	0.9624	Estimated
θ_a	0.8558	Estimated
θ_b	0.0182	Estimated
θ_{ab}	$\theta_a + \theta_b$	Estimated
σ_a	0.0009	Estimated
σ_b	0.9722	Estimated
σ_{ab}	$0.2(\sigma_a + \sigma_b)$	Estimated
δ_a	0.6739	Estimated
δ_b	0.0045	Estimated
δ_{ab}	$\delta_a + \delta_b$	Estimated
γ_a	0.3972	Estimated
γ_b	0.2783	Estimated
γ_{ab}	$0.2(\gamma_a + \gamma_b)$	Estimated
α	0.9996	Estimated
ν_b	0.0048	Estimated
ν_{ab}	ν_{ab}	Estimated
ϕ	0.5000	Estimated
ψ	0.5	Estimated
ρ	0.001–0.5	Estimated
c_1	0.0–1.0	Estimated
c_2	0.0–1.0	Estimated
μ	$\frac{1}{70}$	[8,15]
ξ	0.5	[8,15]

The algorithm used for the model fitting is a built-in MATLAB (R2022b) least-squares fitting routine fmincon in the optimisation tool box. The fitted model reproduces the overall behaviour of the observed data reasonably well. Both the model and the observed data exhibit the same general pattern: a slight decrease in the early years (2000–2003), followed by a modest increase around 2004–2007, a pronounced decline between approximately 2008 and 2017, and finally, a gradual recovery from 2018 onward. This indicates that the model successfully captures the long-term trend of the process being studied. The results of the model fitting given in Figure 2 show that the model (12) is a reasonable fit for the incidence of malaria in Nigeria from 2000 to 2023. Hence, the model is used further for predictions of malaria and its co-infection trends in Nigeria.

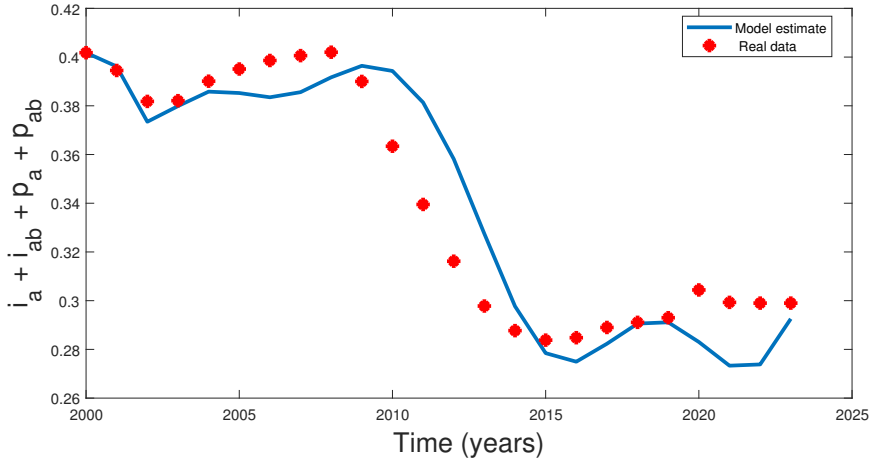


Figure 2. Model fit of the proportion of the incidence of malaria per 1000 population at risk in Nigeria from 2000 to 2023, where bold lines represent the model fit and stars mark the real data.

4.2. Model Predictions

One of the most important aspects of an epidemiological model is its ability to predict outbreaks. Epidemiological models can predict the peak, magnitude, and duration of an infectious disease outbreak, thereby preparing healthcare systems for patient surges and adequate management of the disease. Here, model (12) is used together with the estimated parameters to predict the further possible dynamics of a malaria and typhoid fever epidemic in Nigeria.

Figure 3 is a graphical representation of the long-term dynamics of malaria and typhoid fever co-infection using model (12). The first panel tracks the proportion of the population susceptible to infections. It initially spikes from roughly 0.22 up to 0.35 in the first 5 years, then drops slightly before settling into a long-term multi-year wave pattern. The susceptible population periodically oscillates between troughs of 0.34 and peaks of 0.54, repeating a complex macro-cycle roughly every 24 years.

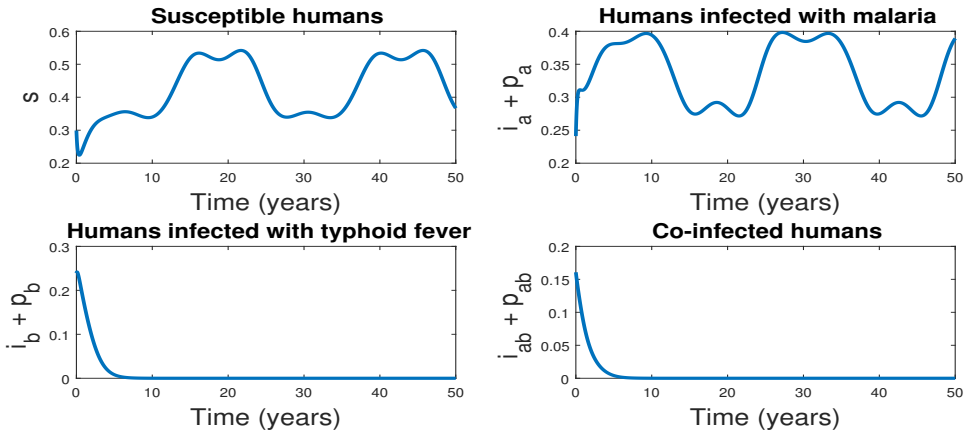


Figure 3. Plot showing the possible long-term dynamics of malaria and typhoid fever co-infection in Nigeria using the estimated parameter values.

For the infected/treated malaria population, we observe from the figure that individuals infected exclusively with malaria (including active infections i_a and treated states p_a) persist. Malaria successfully persists in the population. Mirroring the susceptible curve inversely, malaria infections fluctuate continuously between 0.27 and 0.40 without ever dying out.

Finally, the figures for the infected/treated populations of typhoid fever and co-infection show that both typhoid fever and co-infection will die out in the long-term provided that the control measures are continued to be implemented effectively. This shows that the current control measures considered in this study are capable of eradicating the disease if implemented effectively.

4.3. Effects of Control Measures

The effects of various control measures on the dynamics of the malaria and typhoid fever co-infection model (12) using the estimated parameter values are explored numerically in this section. The results of this analysis are expected to reveal the impact of various control measures in reducing the spread of malaria and typhoid fever co-infection, which is crucial for public health management and disease control.

Figure 4 is a plot showing the effects of the use of mosquito nets (c_1) on the dynamics of the malaria and typhoid fever co-infection model (12) using the estimated parameter values. The figure reveals that use of a mosquito net has significant effects on the numbers of susceptible individuals and humans infected with malaria only, but has less of an effect on the humans infected or co-infected with typhoid fever. This figure shows that increase in the use of a mosquito net decreases the number of malaria-infected humans.

Specifically, effective implementation of the use of mosquito nets leads to eradication of malaria-infected humans in the system. Thus, effective implementation of the use of mosquito nets is strongly recommended for the possible eradication of malaria in the endemic area.

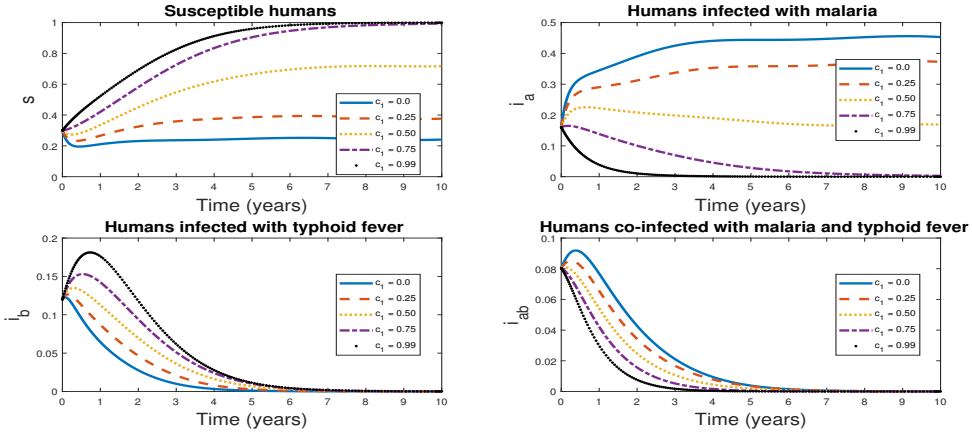


Figure 4. Plot showing the effects of use of mosquito nets (c_1) on the dynamics of the malaria and typhoid fever co-infection model (12) using the estimated parameter values.

Figure 5 is a graphical illustration of the effects of sanitation (c_2) on the dynamics of the malaria and typhoid fever co-infection model (12) using the estimated parameter values. The figure shows that sanitation has significant effects on the population of humans infected with typhoid fever only but has less of an effect on the population of humans infected and co-infected with malaria. This figure also shows that increase in sanitation decreases the number of typhoid-fever-infected humans. Effective implementation of sanitation leads to eradication of typhoid-fever-infected humans in the system. Thus, effective implementation of food, water, and environment sanitation is strongly recommended for the prompt eradication of typhoid fever in the endemic area.

Figure 6 is a plot showing the effects of treatment of malaria only (σ_a) on the dynamics of the malaria and typhoid fever co-infection model (12) using the estimated parameter values. The figure reveals that treatment of malaria only in a co-existence setting has significant effects on the population of malaria-infected humans but no effects on the populations of typhoid-fever- or co-infected humans. Specifically, increasing the treatment rate decreases the population of humans infected with malaria. Thus, effective treatment of malaria alone is strongly recommended for reducing the spread of malaria.

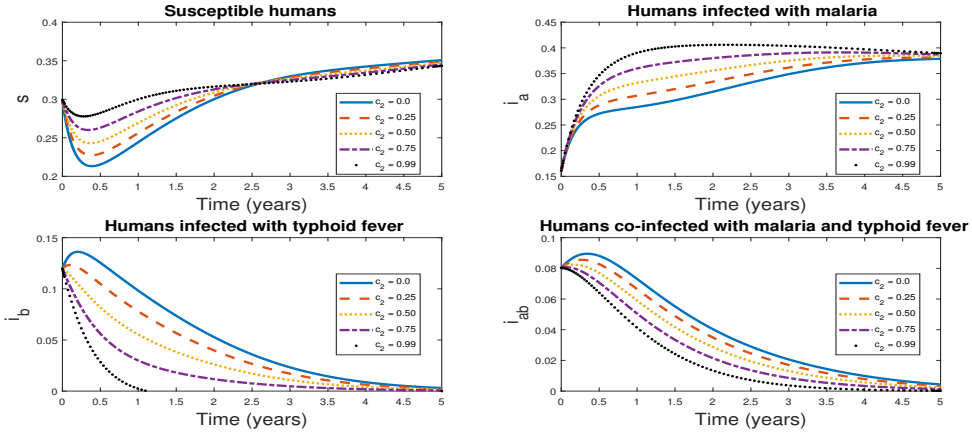


Figure 5. Plot showing the effects of sanitation (c_2) on the dynamics of the malaria and typhoid fever co-infection model (12) using the estimated parameter values.

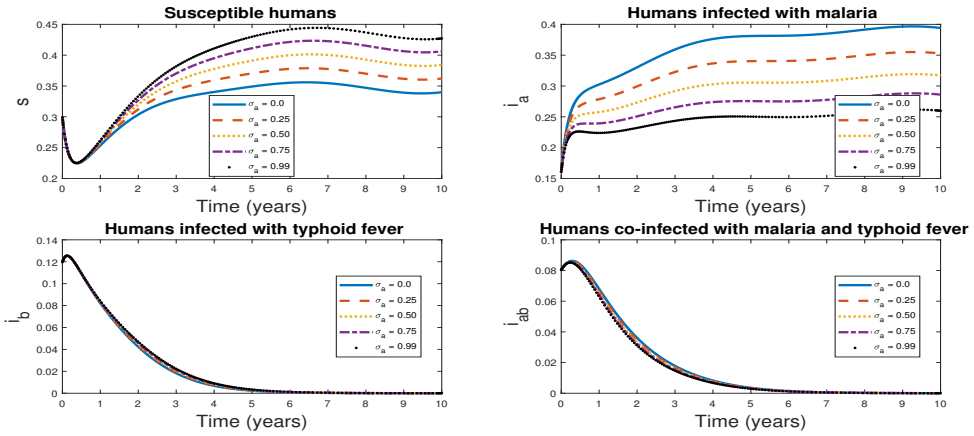


Figure 6. Plot showing the effects of treatment of malaria only (σ_a) on the dynamics of the malaria and typhoid fever co-infection model (12) using the estimated parameter values.

Figure 7 is a plot showing the effects of treatment of typhoid fever only (σ_b) on the dynamics of the malaria and typhoid fever co-infection model (12) using the estimated parameter values. The figure reveals that treatment of typhoid fever only in a co-existence population setting has significant effects on typhoid-fever-infected humans but has minor effects on malaria or co-infected humans. Specifically, increasing the treatment rate decreases the population of humans infected with typhoid fever. Thus, effective treatment for typhoid fever alone is strongly recommended for reducing the spread of typhoid fever.

Now, consider a situation where concurrent treatments are considered in tackling infections in a co-infection setting. Figure 8 is a plot showing the effects of the simultaneous treatment of malaria and typhoid fever on the dynamics of the malaria and typhoid fever co-infection model (12) using the estimated parameter values. The figure reveals that simultaneousness treatment of typhoid fever, malaria, and co-infected humans has significant effects on reducing the number of infected and co-infected humans. By comparing this result with Figures 6 and 7, we observe that simultaneous treatment gives better results. Thus, effective implementation of simultaneous treatment is strongly recommended for reducing the spread of typhoid fever, malaria, and co-infection.

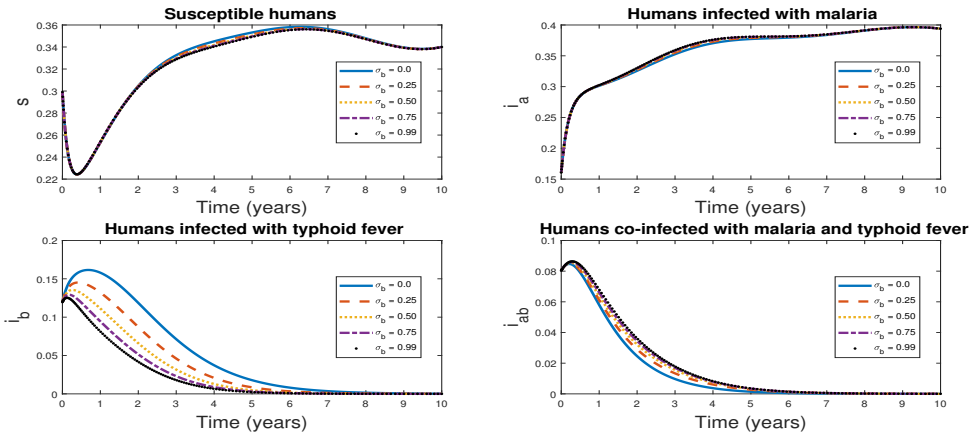


Figure 7. Plot showing the effects of treatment of typhoid fever only (σ_b) on the dynamics of the malaria and typhoid fever co-infection model (12) using the estimated parameter values.

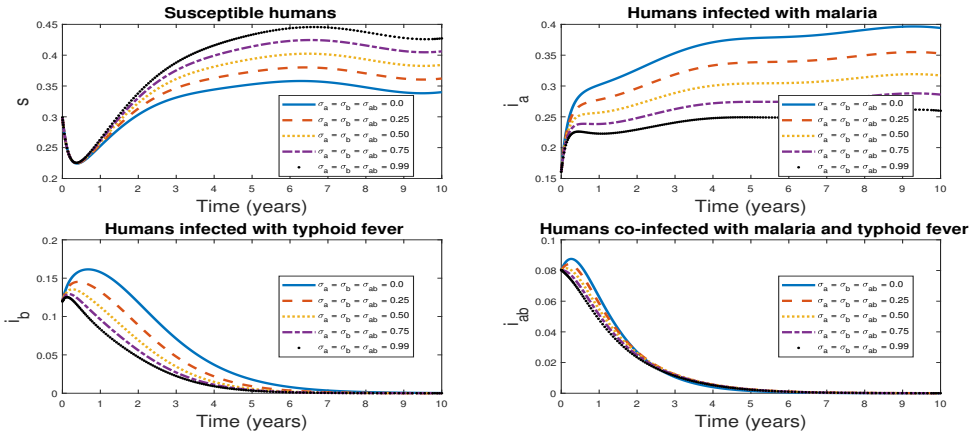


Figure 8. Plot showing the effects of simultaneous treatment of malaria and typhoid fever ($\sigma_a, \sigma_b, \sigma_{ab}$) on the dynamics of the malaria and typhoid fever co-infection model (12) using the estimated parameter values.

Figure 9 is a plot showing the effects of malaria treatment failure (θ_a) on the dynamics of the malaria and typhoid fever co-infection model (12) using the estimated parameter values. The figure reveals that treatment failure on malaria only in a co-existence population setting has some effects on malaria-infected humans but has minor effects on typhoid-fever-infected or co-infected humans. Specifically, an increase in treatment failure leads to an increase in the population of humans infected with malaria. Thus, an effective disease management strategy is strongly recommended for reducing malaria treatment failure.

Figure 10 is a plot showing the effects of typhoid fever treatment failure (θ_b) on the dynamics of the malaria and typhoid fever co-infection model (12) using the estimated parameter values. The figure reveals that treatment failure on typhoid fever only in a co-existence population setting has significant effects on typhoid-fever-infected humans but has minor effects on malaria-infected or co-infected humans. Specifically, an increase in typhoid fever treatment failure leads to an increase in the population of humans infected with typhoid fever. Thus, an effective disease management strategy is strongly recommended for reducing typhoid fever treatment failure.

Now, we consider a complicated situation where there are treatment failures among the various diseases in a co-infection setting. Figure 11 is a plot showing the effects of multiple treatment failure on the dynamics of the malaria and typhoid fever co-infection model (12) using the estimated parameter values. The figure reveals that multiple treatment failures have an impact by increasing the population of humans infected with malaria or typhoid fever as well as those co-infected. Thus, an effective disease management strategy is strongly recommended for reducing treatment failures in a co-infection setting.

Figure 12 is a plot showing the effects of the use of insecticide (ϕ) on the dynamics of the malaria and typhoid fever co-infection model (12) using the estimated parameter values. The figure reveals that using insecticides to kill mosquitoes has a significant impact by decreasing the population of humans infected with malaria, but a minor impact only on decreasing co-infected humans while at the same time enhancing the population of susceptible humans.Thus, effective implementation of the use of appropriate insecticides in killing mosquitoes is strongly recommended for reducing malaria infections.

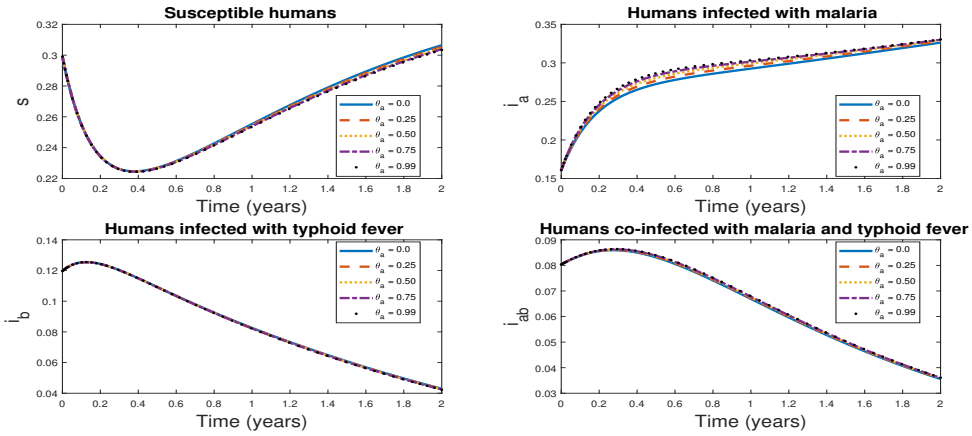


Figure 9. Plot showing the effects of malaria treatment failure (θ_a) on the dynamics of the malaria and typhoid fever co-infection model (12) using the estimated parameter values.

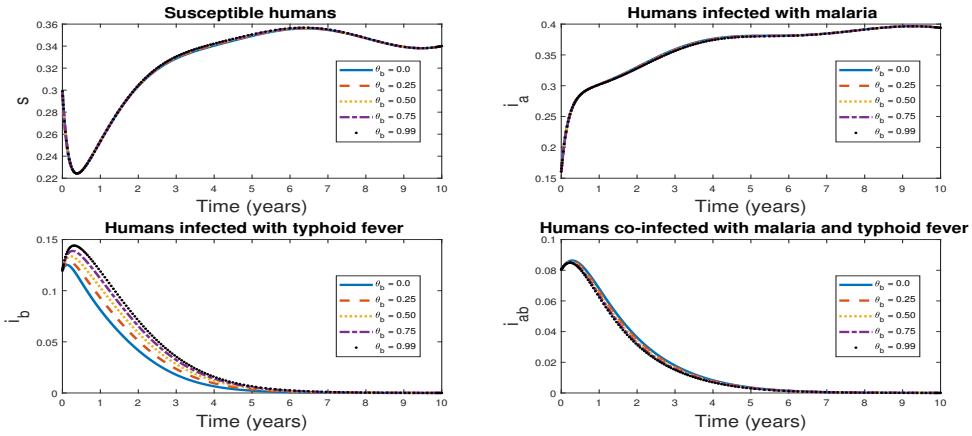


Figure 10. Plot showing the effects of typhoid fever treatment failure (θ_b) on the dynamics of the malaria and typhoid fever co-infection model (12) using the estimated parameter values.

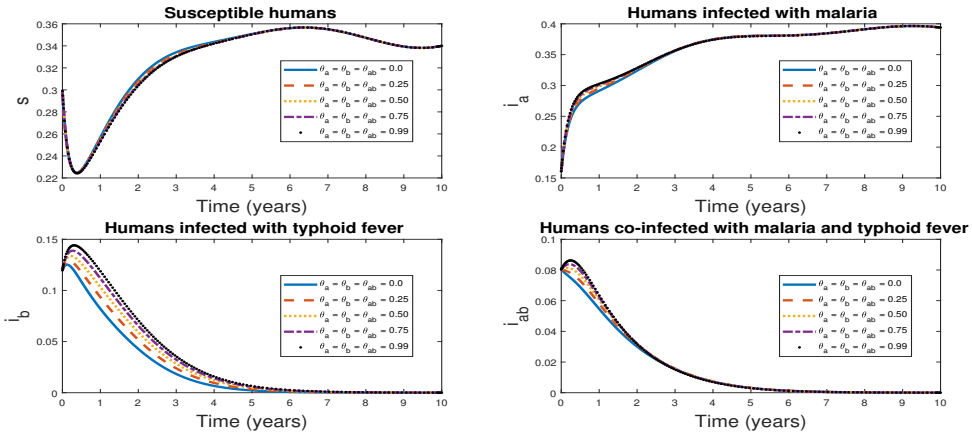


Figure 11. Plot showing the effects of multiple treatment failure ($\theta_a, \theta_b, \theta_{ab}$) on the dynamics of the malaria and typhoid fever co-infection model (12) using the estimated parameter values.

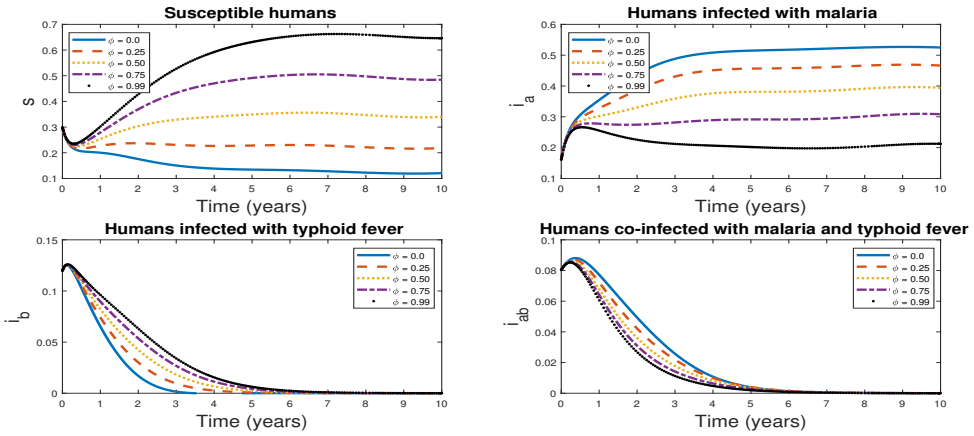


Figure 12. Plot showing the effects of use of insecticide (ϕ) on the dynamics of the malaria and typhoid fever co-infection model (12) using the estimated parameter values.

Figure 13 is a plot showing the effects of bacterial decay due to control interventions (ψ) on the dynamics of the malaria and typhoid fever co-infection model (12) using the estimated parameter values. The figure reveals that bacterial decay due to control interventions has a significant impact by decreasing the population of humans infected with typhoid fever, but has a minor impact on decreasing the population of co-infected humans. Thus, effective implementation of approved control measures that leads to bacterial decay is strongly recommended for reducing typhoid fever infections.

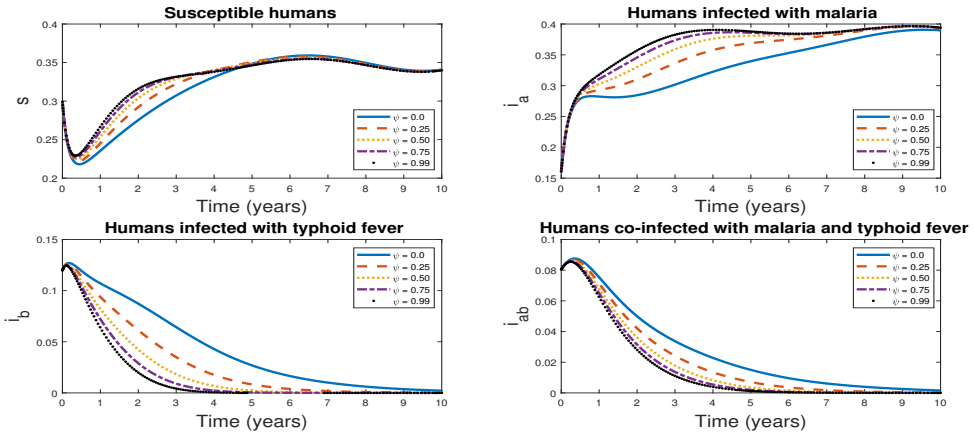


Figure 13. Plot showing the effects of bacterial decay due to control interventions (ψ) on the dynamics of the malaria and typhoid fever co-infection model (12) using the estimated parameter values.

5. Discussion

Malaria and typhoid fever are two severe illness affecting public health. Both diseases are endemic in tropical regions and can severely exacerbate each other where co-infection occurs. In this study, a mathematical model that takes into consideration the essential factors that influence the dynamics and control of malaria–typhoid fever co-infection is developed and analysed accordingly. To estimate the impact of co-infection, a special case of the model where either malaria or typhoid fever is the only sickness affecting the population is extracted from the original model. The epidemiological features of the malaria sub-model and the typhoid fever sub-model such as the basic reproduction number and the equilibrium points are determined. The malaria sub-model and the typhoid fever sub-model were shown to be globally asymptotically stable about the disease-free equilibrium provided that the associated basic reproduction number is less than one. This implies that a malaria or typhoid fever disease outbreak could be eradicated irrespective of the

size of the population of infected humans at the initial stage of the outbreak, provided the control interventions are effective enough to keep the associated basic reproduction number below one. This shows that reducing the associated basic reproduction number below unity through the implementation of effective control measures is sufficient for disease eradication in a situation where either a malaria or typhoid fever outbreak occurs in a population. On the contrary, it was shown that it would be impossible to eradicate malaria–typhoid fever co-infection by lowering the basic reproduction number. This was established theoretically by proving that the malaria–typhoid fever co-infection model is not globally stable about the disease-free equilibrium. This explains why malaria–typhoid fever co-infection is more severe and difficult to eradicate.

Further analysis of the malaria–typhoid fever co-infection model is conducted numerically using data on the incidence of malaria in Nigeria from 2000 to 2023 extracted from [43] as a case study. The results of the model fitting revealed that the malaria–typhoid fever co-infection model (12) is a reasonable fit for the incidence of malaria in Nigeria from 2000 to 2023. Hence, the model is used further for predictions of malaria–typhoid fever co-infection trends in Nigeria. The essential parameters of the malaria–typhoid fever co-infection model (12) were estimated from real data. Model prediction using the estimated parameter values revealed that malaria will remain endemic in Nigeria for a long period unless effective control measures are implemented. On the other hand, typhoid fever and co-infection will die out in the long-term provided that control measures continue to be implemented effectively. The results show that the current control measures considered in this study are capable of eradicating typhoid fever and co-infection if effectively implemented.

The effects of various control measures on the dynamics of malaria–typhoid fever co-infection using the estimated parameter values are explored numerically. For instance, it was shown that increase in the use of mosquito nets decreases the number of malaria-infected humans. Specifically, effective implementation of the use of mosquito nets leads to eradication of malaria-infected humans in the system. Our analysis revealed that increase in sanitation decreases the number of typhoid-fever-infected humans. Effective implementation of sanitation leads to the eradication of typhoid-fever-infected humans in the system. The single treatment of malaria or typhoid fever only in a co-existence setting has significant effects in reducing malaria- or typhoid-fever-infected humans, but has no effects on decreasing the population of co-infected humans. However, the simultaneous treatment of typhoid fever, malaria, and co-infected humans has significant effects on reducing the number of infected and co-infected humans. Thus, effective implementation of simultaneous treatment is strongly recommended for reducing the spread of typhoid fever, malaria, and co-infection. Treatment failure is shown to have a negative impact in the spread of typhoid fever and malaria. However, multiple treatment failure has more of an impact on increasing the population of humans infected with malaria, typhoid fever, as well as those co-infected. Thus, an effective disease management strategy is strongly recommended for reducing treatment failures in a co-infection setting. Further analysis revealed that using insecticides to kill mosquitoes has a significant impact on decreasing the population of humans infected with malaria, but has a minor impact on decreasing co-infected humans while at the same time enhancing the population of susceptible humans. Thus, effective implementation of the use of approved insecticides in killing mosquitoes is strongly recommended for reducing malaria infections. The numerical results revealed that bacterial decay due to control interventions has a significant impact on decreasing the population of humans infected with typhoid fever, but has a minor impact on decreasing the population of co-infected humans. Thus, effective implementation of approved control measures that lead to bacterial decay is strongly recommended for reducing typhoid fever infections.

Finally, this study used a mathematical model to highlight the dynamics and impact of control measures, which is crucial for the proper management of malaria–typhoid fever co-infection. The results of this study are anticipated to aid policy makers and health workers in improving the management of malaria–typhoid fever co-infection in endemic regions for rapid disease eradication.

Author Contributions: Conceptualisation, O.C.C.; methodology, O.C.C.; software, O.C.C. and O.A.O.; validation, O.A.O.; formal analysis, O.C.C.; investigation, O.C.C.; resources, O.A.O.; data curation, O.C.C.; writing—original draft preparation, O.C.C.; writing—review and editing, O.A.O.; visualisation, O.A.O.; supervision, O.A.O.; project administration, O.A.O.; funding acquisition, O.A.O. All authors have read and agreed to the published version of the manuscript.

Funding: This work is based on research supported in part by the National Research Foundation of South Africa (Grant Numbers: 131604).

Data Availability Statement: The original contributions presented in this study are included in the article. Further inquiries can be directed to the corresponding author.

Conflicts of Interest: The authors declare no conflicts of interest.

References

1. Center for Disease Prevention and Control. Clinical Features of Malaria. 2026. Available online: https://www.cdc.gov/malaria/hcp/clinical-features/index.html (accessed on 15 July 2026).
2. World Health Organization. Malaria. 2026. Available online: https://www.who.int/news-room/fact-sheets/detail/malaria (accessed on 15 July 2026).
3. World Health Organization. Typhoid. 2026. Available online: https://www.who.int/news-room/fact-sheets/detail/typhoid (accessed on 15 July 2026).
4. Van den Driessche, P.; Watmough, J. Reproduction numbers and sub-threshold endemic equilibria for compartmental models of disease transmission. *Math. Biosci.* **2002**, *180*, 29–48. [CrossRef]
5. Tien, J.H.; Earn, D.J. Multiple transmission pathways and disease dynamics in a waterborne pathogen model. *Bull. Math. Biol.* **2010**, *72*, 1506–1533. [CrossRef]
6. Collins, O.C.; Duffy, K.J. Mathematical analyses on the effects of control measures for a waterborne disease model with socioeconomic conditions. *J. Comput. Biol.* **2021**, *28*, 19–32. [CrossRef]
7. Castillo-Chavez, C.; Song, B. Dynamical models of tuberculosis and their applications. *Math. Biosci. Eng.* **2004**, *1*, 361–404. [CrossRef]
8. Collins, O.C.; Duffy, K.J. A mathematical model for the dynamics and control of malaria in Nigeria. *Infect. Dis. Model.* **2022**, *7*, 728–741. [CrossRef]
9. Agusto, F.B.; Del Valle, S.Y.; Blayneh, K.W.; Ngonghala, C.N.; Goncalves, M.J.; Li, N.; Zhao, R.; Gong, H. The impact of bed-net use on malaria prevalence. *J. Theor. Biol.* **2013**, *320*, 58–65. [CrossRef]
10. Collins, O.C.; Duffy, K.J. Using data of a Lassa fever epidemic in Nigeria: A mathematical model is shown to capture the dynamics and point to possible control methods. *Mathematics* **2023**, *11*, 1181. [CrossRef]
11. Okuneye, K.; Gumel, A.B. Analysis of a temperature-and rainfall-dependent model for malaria transmission dynamics. *Math. Biosci.* **2017**, *287*, 72–92. [CrossRef]
12. Collins, O.C.; Duffy, K.J. Dynamics and control of mpox disease using two modelling approaches. *Model. Earth Syst. Environ.* **2024**, *10*, 1657–1669. [CrossRef]
13. Zhao, K. A generalized stochastic Nicholson blowfly model with mixed time-varying lags and harvest control: Almost periodic oscillation and global stable behavior. *Adv. Contin. Discret. Model.* **2025**, *2025*, 171. [CrossRef]
14. Kim, J.E.; Choi, Y.; Lee, C.H. Effects of climate change on Plasmodium vivax malaria transmission dynamics: A mathematical modeling approach. *Appl. Math. Comput.* **2019**, *347*, 616–630. [CrossRef]
15. Herdicho, F.F.; Chukwu, W.; Tasman, H. An optimal control of malaria transmission model with mosquito seasonal factor. *Results Phys.* **2021**, *25*, 104238. [CrossRef]
16. Tasman, H. An optimal control strategy to reduce the spread of malaria resistance. *Math. Biosci.* **2015**, *262*, 73–79. [CrossRef]
17. Koella, J.C.; Antia, R. Epidemiological models for the spread of anti-malarial resistance. *Malar. J.* **2003**, *2*, 3. [CrossRef]
18. Mandal, S.; Sarkar, R.R.; Sinha, S. Mathematical models of malaria—A review. *Malar. J.* **2011**, *10*, 202. [CrossRef]
19. Tumwiine, J.; Hove-Musekwa, S.D.; Nyabadza, F. A mathematical model for the transmission and spread of drug sensitive and resistant malaria strains within a human population. *Int. Sch. Res. Not.* **2014**, *2014*, 636973. [CrossRef]

20. Klein, E.Y.; Smith, D.L.; Laxminarayan, R.; Levin, S. Superinfection and the evolution of resistance to antimalarial drugs. *Proc. R. Soc. B Biol. Sci.* **2012**, *279*, 3834–3842. [CrossRef]
21. Kailan Suhuyini, A.; Seidu, B. A mathematical model on the transmission dynamics of typhoid fever with treatment and booster vaccination. *Front. Appl. Math. Stat.* **2023**, *9*, 1151270. [CrossRef]
22. Tsafack, T.J.; Kwa Kum, C.; Tasse, A.J.O.; Tsanou, B. Mathematical modelling of the dynamics of typhoid fever and two modes of treatment in a Health District in Cameroon. *Math. Biosci. Eng.* **2025**, *22*, 477–510. [CrossRef]
23. Khan, I.U.; Mustafa, S.; Shokri, A.; Li, S.; Akgül, A.; Bariq, A. The stability analysis of a nonlinear mathematical model for typhoid fever disease. *Sci. Rep.* **2023**, *13*, 15284. [CrossRef]
24. Dayan, F.; Ahmed, N.; Ali, A.H.; Rafiq, M.; Raza, A. Numerical investigation of a typhoid disease model in fuzzy environment. *Sci. Rep.* **2023**, *13*, 21993. [CrossRef]
25. Lawal, F.; Yusuf, T.; Abidemi, A. On mathematical modelling of optimal control of typhoid fever with efficiency analysis. *J. Niger. Soc. Phys. Sci.* **2024**, *6*, 2057 . [CrossRef]
26. Lawal, F.O.; Yusuf, T.T.; Abidemi, A.; Olotu, O. A non-linear mathematical model for typhoid fever transmission dynamics with medically hygienic compartment. *Model. Earth Syst. Environ.* **2024**, *10*, 6213–6232. [CrossRef]
27. Alalhareth, F.K.; Alharbi, M.H.; Ibrahim, M.A. Modeling typhoid fever dynamics: Stability analysis and periodic solutions in epidemic model with partial susceptibility. *Mathematics* **2023**, *11*, 3713. [CrossRef]
28. Nana-Kyere, S.; Kiddy K.; Asamoah, J.; De-Graft Ankamah, J.; Okyere, E.; Seidu, B.; Kwarteng, D.; Ayetey, E.L.; Kwabena Odum, J. Mathematical Modeling and Cost-Effectiveness Analysis of an SEIR Typhoid Fever Model. *J. Math.* **2025**, *2025*, 1212057. [CrossRef]
29. Tilahun, G.T.; Makinde, O.D.; Malonza, D. Modelling and optimal control of typhoid fever disease with cost-effective strategies. *Comput. Math. Methods Med.* **2017**, *2017*, 2324518. [CrossRef]
30. Tijani, K.A.; Madubueze, C.E.; Gweryina, R.I. Modelling typhoid fever transmission with treatment relapse response: Optimal control and cost-effectiveness analysis. *Math. Model. Comput. Simulations* **2024**, *16*, 457–485. [CrossRef]
31. Bakach, I.; Just, M.R.; Gambhir, M.; Fung, I.C.H. Typhoid transmission: A historical perspective on mathematical model development. *Trans. R. Soc. Trop. Med. Hyg.* **2015**, *109*, 679–689. [CrossRef]
32. Sanda, A.; Odekunle, M.R.; Momoh, A.A.; Dione, D. On the modeling and stability analysis of fractional typhoid fever model with optimal control. *Results Control Optim.* **2025**, *19*, 100552. [CrossRef]
33. Sohanang Nodem, F.S.; Ymele, D.; Fadimatou, M.; Fodouop, S.P.C. Malaria and Typhoid Fever Coinfection among Febrile Patients in Ngaoundéré (Adamawa, Cameroon): A Cross-Sectional Study. *J. Parasitol. Res.* **2023**, *2023*, 5334813. [CrossRef]
34. Olowolafe, T.A.; Agosile, O.F.; Akinpelu, A.O.; Aderinto, N.; Wada, O.Z.; Olawade, D.B. Malaria and typhoid fever co-infection: A retrospective analysis of University Hospital records in Nigeria. *Malar. J.* **2024**, *23*, 220. [CrossRef]
35. Odikamnoro, O.O.; Ikeh, I.M.; Okoh, F.N.; Ebiriekwe, S.C.; Nnadozie, I.A.; Nkwuda, J.O.; Asobie, G.C. Incidence of malaria/typhoid co-infection among adult population in Unwana community, Afikpo north local government area, Ebonyi state, Southeastern Nigeria. *Afr. J. Infect. Dis.* **2018**, *12*, 33–38. [CrossRef]
36. Ahman, Q.O.; Okofu, M.B.; Ejikeme, C.L.; Senewo, E.O.; Agbata, B.C. Mathematical Modeling of Malaria and Typhoid Co-infection: Exploring Vector and Non-Vector Transmission Dynamics. *Math. Model. Nat. Phenom.* **2026**, *21*, 12. [CrossRef]
37. Mutua, J.M.; Wang, F.B.; Vaidya, N.K. Modeling malaria and typhoid fever co-infection dynamics. *Math. Biosci.* **2015**, *264*, 128–144. [CrossRef]
38. de Souza Mendes, P.R. Dimensionless non-Newtonian fluid mechanics. *J.-Non-Newton. Fluid Mech.* **2007**, *147*, 109–116. [CrossRef]
39. Malekjani, N.; Kharaghani, A.; Tsotsas, E. A comparative study of dimensional and non-dimensional inputs in physics-informed and data-driven neural networks for single-droplet evaporation. *Chem. Eng. Sci.* **2025**, *306*, 121214. [CrossRef]
40. Castillo-Chavez, C.; Feng, Z.; Huang, W. On the computation of R_0 and its role on global stability. In *Mathematical Approaches for Emerging and Reemerging Infectious Diseases: An Introduction*; Springer: New York, NY, USA, 2002 ; Volume 125 .
41. Akinyemi, K.O.; Oyefolu, A.O.B.; Mutiu, W.B.; Iwalokun, B.A.; Ayeni, E.S.; Ajose, S.O.; Obaro, S.K. Typhoid fever: Tracking the trend in Nigeria. *Am. J. Trop. Med. Hyg.* **2018**, *99*, 41. [CrossRef]
42. Kehinde, A.; Ogunleye, V.; Popoola, O.; Amadi, E.; Coker, A.; Rahman, M.; Akintunde, Y.; Adebiyi, I.; Ogundairo, J.; Otunla, E.; et al. Seasonal patterns in typhoid environmental surveillance in Ibadan, Nigeria. *Int. J. Infect. Dis.* **2025**, *152*, 107386. [CrossRef]
43. World Health Organization. Incidence of Malaria (per 1000 Population at Risk)—Nigeria. Global Health Observatory Data Repository/World Health Statistics. Available online: https://data.worldbank.org/indicator/SH.MLR.INCD.P3?locations=NG (accessed on 15 January 2026).

Disclaimer/Publisher's Note: The statements, opinions and data contained in all publications are solely those of the individual author(s) and contributor(s) and not of MDPI and/or the editor(s). MDPI and/or the editor(s) disclaim responsibility for any injury to people or property resulting from any ideas, methods, instructions or products referred to in the content.